5-2015

Simulation of a Dissimilar Fresnel Relfectarray Antenna

Paul L. Rogers
University of Arkansas, Fayetteville

Simulation of a Dissimilar Fresnel Reflectarray Antenna

An Undergraduate Honors College Thesis

In the

Department of Electrical Engineering

College of Engineering

University of Arkansas

Fayetteville, AR

By

Paul Leeds Rogers III

This thesis is approved.

Thesis Advisor:

_____

Thesis Committee:

_____

_____

Abstract

Planar reflectarray antennas behave similarly to parabolic dish antennas, but are flat in their construction. They work by having areas on the planar surface of different reflection phase, causing the signal to be reflected to a focal point. This is done today by making planar patch antennas with the required reflection phase. These antennas are typically used in aerospace. This paper specifically discusses a planar reflectarray antenna that was originally constructed in Millimeter Wave Circularly Polarized Fresnel Reflector for On-Board Radar on Rescue Helicopters by K. Mazouni. In this paper, the authors eight different shaped antennas to form the planar reflectarray. The typical planar reflectarray would use eight variations on the same patch to achieve the required performance. This paper recreated the results of the simulations of the unit cell patches.

Acknowledgements

This work was supported in part by the National Science Foundation under grants MRI #0722625, MRI-R2 #0959124, and #0918970.

Table of Contents

List of Figures

List of Tables

List of Equations

1. Introduction

When designing an antenna, there are many forms that you have to choose from. There is the dipole antenna, a standard antenna consisting of two wires; there is a patch antenna, which is a thin strip of conductor sitting on top of a substrate; there is a Yagi-Uda antenna, which is an antenna composed of several dipole antennas of different sizes connected to the same feed; and there is the dish antenna, which works by focusing incoming signals to a small antenna located at the focal point of the dish. Each of these different designs has different properties that make each design more desirable in different instances. Before discussing the advantages of each, it would be important to consider what an antenna is.

An antenna is a structure used to radiate electromagnetic waves. This is in contrast to the other method of transmitting electromagnetic waves: transmission lines. In a transmission line, the waves and their associated energy are contained within the line, which could be a wire or a strip of conducting metal. Antennas radiate electromagnetic waves without confinement. [**1**]

An antenna radiates waves due to the currents inside of its conducting structure. Consider a single charged particle; when it is at rest, it has field lines pointing to infinity. Regardless of where this charged particle is, it will have these lines to infinity. If we consider what happens when the particle moves, the field lines before and after the movement are pointing radially away from the particle. Because we cannot have a discontinuity in these field lines, there is a distortion in the field between the "before movement" lines and the "after movement" lines. This distortion is radiation, and propagates away from the charge at the speed of light. If the comparison with a

stone thrown into a body of water is used, then the movement of the charge is the same as the stone hitting the water. [**1**]

Most antennas do not have charges moving in just one direction, most have an oscillating current running through them. Consider a short length of wire fed by an oscillating current source: before the charges start moving, the wire is not polarized, so there are no field lines. A short time after the current source is turned on, one side of the wire will have a concentration of positive charge and the other side will have a concentration of negative charge. At this moment, there will be field lines pointing from the positive to the negative end. A moment later, the current reverses direction and the charge distribution is even again. At this moment, there are no field lines coming from the wire, but the lines that were there already do not just disappear. Those lines became closed as the charge distribution neutralized, producing a displacement current in space. As the charges build up at the ends of the wire again, the cycle starts anew. As long as the current source continues to produce the alternating current, the radiation will be continuous. It is important to note that in real antennas, charges do not flow and build up as in this example, but merely displace enough to pass energy to their nearest neighbor charge. The original description is convenient and produces the same result. [**1**]

In [**1**], antennas are broken up into four different types: electrically small, resonant, broadband, and aperture antennas. Electrically small antennas are antennas with significantly less than a wavelength in length, where construction does not affect the behavior of the antenna much. Resonant antennas are simple antennas or arrays of antennas that operate well at single or narrow frequency bands. Broadband antennas have consistent performance over a wide range of

frequencies. Aperture antennas have a physical aperture that “funnels” waves. In order to properly compare these antenna types, antenna properties must be discussed.

The most important antenna properties are radiation pattern, directivity, gain, polarization, impedance, and bandwidth. Radiation pattern is the shape of the radiation intensity around the antenna. Directivity is the ratio of the peak power of the antenna to the average power output of the antenna. A high directivity antenna will have one main beam with some small side beams, and a small directivity antenna will have either multiple main beams or one main beam with large side beams. The gain of an antenna is the directivity of the antenna reduced due to losses in the antenna. Polarization is the shape traced out by the electric field vector if looked at through time. As the electrical signal travels through space, the wave may have components in the x and y dimensions of a plane. If all of the magnitude of the electric field is in the x or y direction, then the antenna is said to be linearly polarized. If the magnitude of the electric field is in the x and y directions equally, then the antenna is said to be circularly polarized. If the magnitude of the electric field is different in the x and y directions, the antenna is said to be circularly polarized. Impedance is the same as electrical impedance, and refers to the resistance and associated phase shift of the component. The bandwidth of an antenna is the range of frequencies over which all of the parameters are considered acceptable. [**1**]

Now that the parameters are described, the different kinds of antennas can be compared. Electrically small antennas typically have a low directivity, input resistance, and gain, along with high input reactance. Resonant antennas typically have low gain and a narrow bandwidth, but a real impedance. The real impedance allows them to be more easily matched to transmission lines

to increase efficiency. Broadband antennas have low but constant gain, real impedance, and a wide bandwidth. Aperture antennas have high gain and moderate bandwidth. [**1**]

Most people are familiar with aperture antennas, as parabolic reflector antennas are in this category. These antennas have a parabolic dish that reflects incoming signals to a smaller feed component placed at the reflector's focal point. Like most aperture antennas, they typically have very high gain and as such are used in areas such as space communication [**2**]. The downside to using these antennas in space, and other, applications is that they are rather high volume. There is another type of reflecting antenna similar to a parabolic dish antenna, but the reflector is flat. [**2**]

The planar reflectarray antenna (PRA) works on the same principal as the dish antennas, but uses an array of antennas, either waveguides [**3**] or more commonly microstrip antennas, to reflect the incoming waves to a focal point. Since the reflective surface is comprised of discreet reflective elements instead of a continuous reflective surface, the gain of PRAs is not as high as parabolic dish antennas. Some of the biggest reasons people may prefer a PRA to a parabolic dish antenna is that PRAs are more easily manufactured since they use printed circuit/antenna fabrication [**2**], the size and shape of PRAs are usually smaller and more flexible than dish antennas making them more attractive for space applications [**2**], and PRAs can be designed to have a variety of beam shapes or to even have electronic scanning instead of mechanical scanning [**2**] [**4**]. All of these benefits are because the PRA is made up of an array of patches.

Most PRAs consist of variations on a single type of patch, such as several rectangles with different widths or with different lengths of feed line, providing the reflective surface [**2**] [**5**] [**4**] [**6**] [**7**] [**8**]. In [**9**], the authors designed a PRA that used entirely dissimilar unit cells to make up

the reflective surface of the antenna. The goal of this paper is to examine the design of these unit cells and recreate the results of each cell in that paper.

A. Literature Review

This section describes the literature in chronological order, with the latest paper reviewed first and the most recent paper reviewed last.

The Reflectarray Antenna by D.G. Berry

This article marks the first appearance of the concept of reflectarray antennas. The author computes the required surface impedance function that would allow one to generate a desired reflected beam shape. The author provided two methods of realizing this function: exact matching of the impedance function, and approximation of the impedance function. The exact matching implementation would be accomplished by placing a varying thickness metal on top of a dielectric. The approximation implementation would be implemented as an array of discreet elements. At the time, the technology for printed antennas was not mature, so the author used dipoles and shorted waveguides as examples of these discreet elements. The author then goes to construct three different reflectarray antennas based on the surface impedance function. One of them is an array of regularly spaced waveguides with varying shorted depths, one is the same but with staggered rows, and one was a shorted waveguide design designed for circular polarization. The author shows that each of these performed as expected. The author also proposed an advantage to the reflectarray antenna concept: electrical control. Each of the individual antennas in the array could be connected to some kind of electronic controller allowing electrical beam control, including sweeping and changing the beam shape. [**3**]

U.S. Patent 4 684 952 by Munson et al.

This is the first instance of a reflectarray antenna using planar microstrip antennas. In this patent, the authors describe the advantages of PRAs over parabolic dish antennas, including mechanical advantages and simple manufacture. The authors then describe some possible uses for the PRA including making an object have a larger or smaller radar cross section. The rest of the document details specific designs that the authors patented. [**2**]

Flat Printed Reflector Antenna for mm-Wave Applications by B. Huder

This paper deals with the design of a Fresnel reflector antenna. In optics, Fresnel reflectors are mirrors that reflect visible light either into a focal point or from a focal point into a beam using a relatively flat mirror instead of a curved one. This paper shows that the Fresnel technique of dividing a reflector into concentric circles of different phase provides a working antenna, even if it doesn't have gain as good as a parabolic reflector. [**10**]

Design of a Millimeter Wave Microstrip Reflectarray by D. M. Pozar

This paper goes into detail with the theoretical modeling of PRAs and practical modeling. The author derives the plane-wave reflection from a uniform, infinite array. The solution is then used to design an antenna. Four designs were built and tested, showing that the design method worked for both 28 and 77 GHz. [**5**]

A Shaped-Beam Microstrip Patch Reflectarray by D.M. Pozar

This paper discusses the design of a shaped-beam PRA, as most papers before this one focused solely on pencil beam PRAs. The outline of the PRA was decided upon by using a

previously designed shaped-beam antenna that was not a PRA. This shape was put into a program to determine the contours of constant reflection phase, allowing the authors to place the specific unit cells in the correct locations. The paper concludes with the PRA being inferior to the original shaped-beam antenna, but the authors think the tradeoffs may be worth the easy in manufacturing of the PRA. [**4**]

A C/Ka Dual Frequency Dual Layer Circularly Polarized Reflectarray Antenna with Microstrip Ring Elements by C. Han et al.

This paper discusses the design of a circularly polarized reflectarray. Interestingly, none of the individual elements of the antenna are themselves circularly polarized. The authors obtained circular polarization by rotating the individual patches. The design also incorporates a dual layer technology, making the antenna size significantly smaller. The dual layer layout allows two different sized patches to be used in the design, allowing the antenna to operate at two different frequency ranges. [**6**]

94 GHz Folded Fresnel Reflector Using C-Patch Elements by B.D. Nguyen et al.

This paper discusses a folded reflector antenna, which had a similar structure to the antenna in the previous article: dual layered. In this design, the secondary layer is actually a semi-reflecting grid whose purpose is to redirect the signal from the feed to the primary layer and have the reflection off the primary layer pass through the secondary layer. The individual patches used in this design were C shaped patches. The authors discuss the design of the C-cells, starting with a ring patch. They plotted the current density of the ring patch, showing the areas of maximum and minimum current. The minimum current was found to be where the patch crossed the axis the electric field was polarized to. When they cut a slot out of the ring in the area of minimum

current when the electric field was y-polarized, they found the electric field almost unchanged. They then kept the same geometry but switched the field to x-polarization. They found that this slot caused a phase change in the reflected field. They then found that changing the width of the slot changed the reflected x-polarization phase and not the y-polarization phase.

The paper then goes to discuss the simulation setup for the design. Using Ansoft-HFSS, they simulated the patches as if they were a unit cell in an infinite periodic array. This was done by placing electric and magnetic walls around the patch, with the electric field perpendicular to the electric walls. To obtain a baseline phase reflection, the height of the simulation box was adjusted so that the reflected phase of an entirely metallic cell was 0º. The y-polarization reflection was then optimized to the Fresnel zone, and the x-polarization was optimized for a 180º phase difference.

The antenna was fabricated and then tested. The results corresponded with the expected results based on the simulation results. The antenna itself was determined to be very sensitive to manufacturing errors. [**7**]

Millimeter Wave Circularly Polarized Fresnel Reflector for On-Board Radar on Rescue Helicopters by K. Mazouni

This is the article that this paper is attempting to recreate. The design of their antenna is broken into two parts: design of a Fresnel reflector and elementary cell design. Both of these will be discussed in more detail in the Methodology chapter, but a basic overview is that Fresnel reflector design describes the phase shift necessary to transform a parabolic reflector to a planar reflector with similar properties. The elementary cells need to fit the phase shift required by the Fresnel design and to produce a circular polarization from a linear excitation.

There were two parts to the simulation of the unit cells: obtain desired phase shift and polarization through the periodic structure model, and check circular polarization by using Master-Slave simulation with a linearly polarized excitation at 45º to the walls. The original unit cell design was a series of variations on the C-cell design of the previous paper; however, the fabrication technology was not accurate enough to produce the fine design changes in the cells. The minimum dimension within a patch was 100μm. The authors decided to use a collection of dissimilar cells, meaning that each phase compensation zone had a unique patch that was not a simple variation on another patch's geometry. There were three types of geometry discussed: variations of the C-cell, rectangular patch, and offset patches. The variations of the C-cell included making additional cuts into the C patch, leading to things such as two crescents forming the antenna and an antenna that was similar in shape to a cartoon bat. The rectangular patches were conceived similarly to the C-cell variations: the authors took a basic rectangular patch and removed pieces of the antenna to achieve the desired results. The offset patches were strangely shaped patches that were offset from the center of the unit cell. The authors describe this as the first application of offset patches for printed reflector use.

When describing the antenna performance, the authors provided two measurements of their antennas. First was axial ratio. It should be noted that the authors use a different definition of axial ratio than is typical in antenna design. The authors describe this as the ratio of the maximum and minimum reflected field. In typical antenna design, axial ratio is the ratio of the x and y polarizations of the electric field. The typical definition results in an axial ratio of unity when the electric field is circularly polarized, and the authors' description is unity when the minimum and maximum electric fields are the same. The authors never discuss the reason for changing the definition, but it may be that the new axial ratio describes producing a uniform

plane wave as the reflected field. The other measurement used to describe the patches is $\Delta\Phi^o$, defining the difference between the y-phase and the x-phase.

The antenna is then fabricated using the individual patch designs. The fabricated antenna is considered acceptable by the researchers even though the results are slightly worse than previous results. The authors state that the poorer performance is offset by the circular polarization of the antenna. [**9**]

Folded Reflectarrays with Shaped Beam Pattern for Foreign Object Debris (FOD) Detection on Runways by A. Zeitler

One of the previously mentioned advantages of PRAs compared to a dish antenna is the ability to design a PRA to have a specific beam shape. In this paper, the authors designed a PRA with an altitude pattern of cosecant squared and a pencil beam in the azimuth. The authors state that the cosecant squared pattern is necessary for a constant received power within a distance range. The azimuthal pencil beam was used because the antenna would be scanned mechanically. The authors derive a one- and two-dimensional solution for the phase distribution of the antenna, with the one dimensional analysis to assist the two-dimensional solution. The authors used the open-source software Scilab to optimize the antenna design. The unit cells were designed and optimized in Ansoft-HFSS using the periodic structure model. The results of the individual patch designs were imported to Scilab and used to simulate the full antenna radiation pattern. The fabricated antenna matched the simulated results, showing that the technique used for design was good. [**11**]

77 GHz FM-CW Radar for FODs detections by K. Mazouni

This paper is an extension of the previous. It combines the previous antenna design with a radar module in an attempt to show that the antenna's performance matches the FOD detection specifications set by the Federal Aviation Administration (FAA). The antenna used is exactly the same as described in the previous paper. The paper also discusses the design and performance of the radar module, showing that it performs well in the frequency range (76-81 GHz) of the antenna. One of the differences with this design and existing systems was that this design was broadband, 5 GHz, while the existing system's bandwidth was only 1 GHz. The results of the measurements show that there was a significant improvement in performance by using a broadband system in comparison with a small band system. [**12**]

77 GHz offset reflectarray for FOD detection on airport runways by K. Mazouni

This paper is also a continuation of the previous two papers. The authors state that while the previous antenna design worked well at short distances, the design did not meet FAA specifications for sensitivity at range. They also noted that in the results, circular polarization did not offer any tangible benefit over linear polarization. Thus, the antenna designed in this system was a linearly polarized antenna. The authors claim that the antenna is intended to operate in the same 76-81 GHz band as the previous, but only the 76-77 GHz results are shown.

The antenna in this paper was designed similarly to other PRAs. The unit cell patches were rectangles with different lengths and widths to provide the necessary reflection phases. The simulation of the unit cells was different in this paper because they used the Floquet port method in Ansoft-HFSS to obtain the simulation results. This allowed for all polarization results to be obtained in a single simulation profile instead of several as described in previous papers. The full

antenna was also simulated after the unit cells were designed, but the results were only accurate in the main lobe due to some approximations made.

The antenna was then fabricated and tested, showing results near, but not quite meeting, the specification requirements. The authors believe this is because the maximum gain of the antenna was measured to be around 78.5 GHz, which was outside of the radar testing frequencies. The authors state that a new radar module being designed would allow for optimal testing conditions. [**8**]

2. Methodology

This chapter provides an overall view of the methodology of this paper. The first section describes Fresnel reflectors and the operation of PRAs, while the second section describes the simulation process for the unit cells of the PRA described in [**9**]. All simulations done for this research were performed on the supercomputer maintained by the Arkansas High Performance Computing Center (AHPCC) at the University of Arkansas.

B. Fresnel Reflector and PRA Operation

Many of the PRA designs seen today in the literature are described as "Fresnel type" [**6**] [**7**] [**8**] [**9**] [**12**]. A Fresnel reflector is a planar reflector that behaves similar to a parabolic or spherical reflector in that it has a focal point where it focuses incoming light/signals [**10**]. The phase compensation of a Fresnel zone is defined in Equation 1. This equation says that the reflector is made up of concentric circles of constant phase, with P being the number of zones, k being the number of the zone being described, and Φ_k being the phase of that zone.

$$\Phi_k = 2\pi \frac{k-1}{P}, k \in [1, P] \text{ [9]}$$ Equation 1

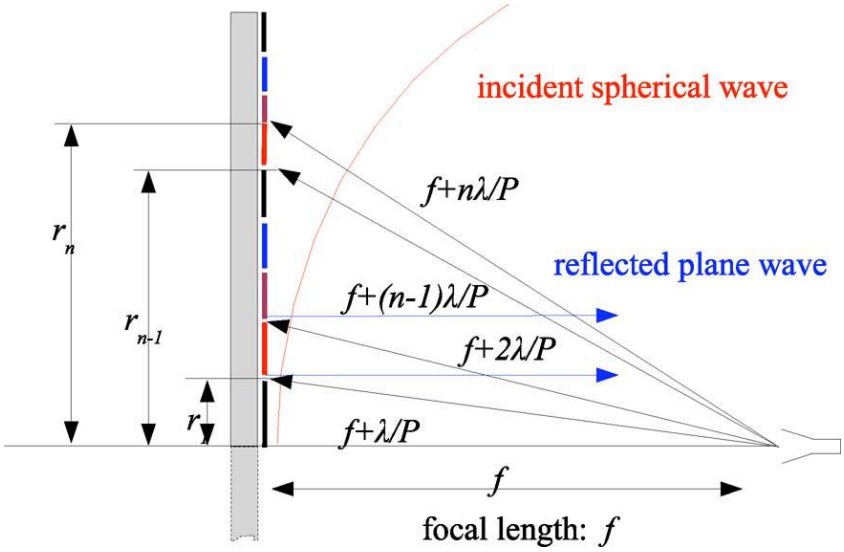

Figure 1: Fresnel reflector geometry, found in [**9**]

In order to find the inner and outer radii of these concentric circles of constant phase, the geometry must be considered. The geometry of a Fresnel reflector can be seen in Figure 1. To calculate the length of r_n, simple trigonometry is used:

$$r_n^2 + f^2 = \left(f + \frac{n\lambda}{P}\right)^2$$ Equation 2

$$r_n^2 + f^2 = f^2 + \frac{2nf\lambda}{P} + \left(\frac{n\lambda}{P}\right)^2$$ Equation 3

$$r_n^2 = \frac{2nf\lambda}{P} + \left(\frac{n\lambda}{P}\right)^2$$ Equation 4

$$r_n = \sqrt{\frac{2nf\lambda}{P} + \left(\frac{n\lambda}{P}\right)^2} \text{ [7]}$$ Equation 5

In Equation 2-5 and in Figure 1, r_n is the nth radius, n is the current radius number, f is the focal point distance, λ is the wavelength of the design frequency, and P is the order of phase compensation, i.e. the number of different phase zones. If there were eight different phases that were being considered in the design, then the order of phase compensation would be eight. One thing to note about this equation is that the difference $r_n - r_{n-1}$ decreases as the n increase and as P increases. To compensate for this shrink in the spacing, some researchers have decreased the order of phase compensation as the radius increases [**7**] [**9**]. This increases the size of the Fresnel zone.

Using Equation 5 to determine the radius sizes, there is now a description for the layout of an antenna with phase order P. In [**9**], the authors decide on a phase order of eight, meaning that there are eight different phases: 0°, 45°, 90°, 135°, 180°, 225°, 270°, and 315°. As discussed before, the authors of [**9**] originally intended each of these reflection phases to be generated by a single variation on a C-cell. The authors found that the fabrication techniques that they would use were not accurate enough to produce these variations [**9**], and so the authors decided to work with a collection of dissimilar patch shapes, which can be seen in Figure 2.

While the dimensions for each patch were not given, the dimensions for the substrate were given: 254 μm thick copper-clad Duroid substrate with a relative permittivity of 2.2. Each of the unit cells was $\frac{\lambda}{2}$ square, and the solution frequency was 78 GHz. This paper focused on recreating the simulation results for each of these patches. The characteristics of each patch are described in Table 1. The axial ratio in this table is defined as the ratio of the maximum and

minimum electric field and the ΔΦº is defined as the difference between the y-polarization reflection phase and the x-polarization reflection phase.

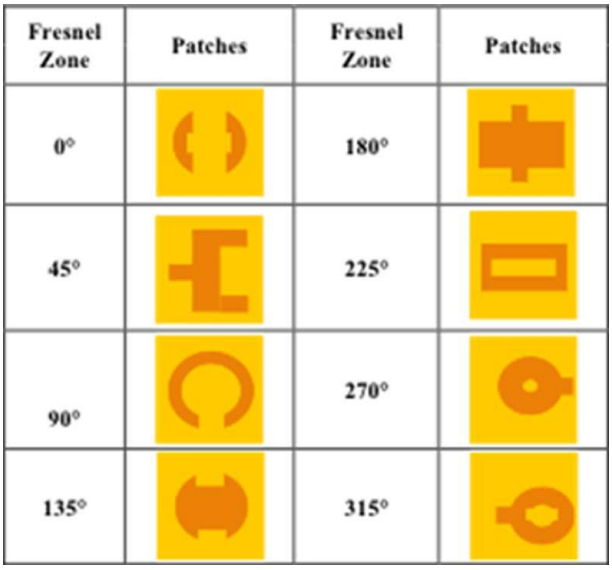

Figure 2: Patch antennas with phase compensation zones, found in [**9**]

Table 1: Simulated results from the patches in Figure 2 from [**9**]

Fresnel zone	0°	45°	90°	135°	180°	225°	270°	315°
AR (dB)	0.4	0.6	0.6	0.14	0.5	0.07	0.33	0.22
$\Delta\Phi$ °	89	86	89	89	93	90	88	92
CP	RHCP							

C. Simulation Process

The simulation process took place in Ansoft-HFSS, a computational electromagnetics solver that uses finite element analysis to solve Maxwell's equations everywhere in the domain. Finite element analysis means that the domain is broken down into small tetrahedra, four-sided polygons, forming a mesh inside the domain. The software then solves Maxwell's equations on

the vertices and in the middle of the faces of these tetrahedra. Since this is a numerical solution, there will be error in the solution. To check that the solution found is acceptable, the software takes the initially created mesh and refines it such that the existing tetrahedra are broken into multiple smaller tetrahedra. After the software obtains a solution for the new mesh, it compares the two solutions to the volume. If the relative error between the two is below an acceptable error as set by the researcher, the solution has converged and the software uses the existing mesh and solution as the final solution. If the relative error is higher than what the researcher set, then the software repeats the mesh refinement until the solution has converged. In Ansoft-HFSS, the researcher can set the maximum number of passes and the convergence criteria, called ΔS. For this paper, the maximum number of passes was 30 and the ΔS was set to 0.001. The solution frequency, the frequency at which the design is intended to operate, was set to 78 GHz.

The method used in [**9**] to characterize the patch antennas was called the infinite periodic array. The patch, substrate, and ground plane were placed inside a vacuum geometry the same length and width, with the bottom of the vacuum geometry touching the bottom of the ground plane. The infinite periodic array configuration involves placing the patch between two parallel electric walls and two parallel magnetic walls. The electric walls are perpendicular to the magnetic walls. The unit cell then has the excitation set up as a uniform plane wave polarized perpendicular to the electric walls. As an example, to make a cell for testing the x-polarization response, the two walls of the vacuum geometry perpendicular to the x-axis need to be made electric walls and the two parallel to the x-axis need to be made magnetic walls. The plane wave needs to be x-polarized. This simulation technique treats the unit cell as if it were in an infinite periodic array of the same shape as the unit cell. An issue in this technique is that in a real life situation the patch would not be surrounded by patches of similar shape but of different shape.

This effect is described as negligible due to minimal mutual coupling between thin microstrip substrates in [**5**].

In order to properly compare reflected phase between these patches, a suitable measuring height needed to be established. This was accomplished through a method described in [**7**]. A rectangular prism of metal the same height, width, and length of a final patch was created and set up as described in the previous paragraph. The height of the vacuum geometry was then optimized to provide an S11 phase of 0°. The resulting height was used in every simulation to ensure comparability of S11 phase across all of the simulations.

Each of the patches to be simulated had a relatively complex geometry. If the individual cells were put through the built in optimization program in HFSS with each of the geometry variables, the time taken to simulate each cell would be very large. The individual cells and their dimension names used in simulation can be seen in Figure 3 to Figure 10. To shorten this time, an initial survey of the ways the different geometric variables affected the reflected phase was done. The goal of these surveys was to see if there were any geometric variables that caused minimal changes in reflection phase. If any were found, they were left out of the optimization step.

The next step of the design and simulation was to obtain a single patch as a reference patch around which to design the other patch reflection phases. The y-polarization of the patches was used to meet the Fresnel zone phase requirement. The x-polarization was used to determine circular polarization. In this case, the 0° patch design was chosen as the reference patch. When the phase of this patch was found, the remaining patches could be designed for a reflected phase with that patch as a reference.

Once the 0° reference phase was found, the other shapes were put through the optimization algorithm built into Ansoft-HFSS. The goal was to get the S11 phase at 78 GHz to be the 0° reference phase plus the Fresnel zone frequency for that patch. The variables selected for the optimization algorithm were limited to those found in the previous step to influence reflection when changed.

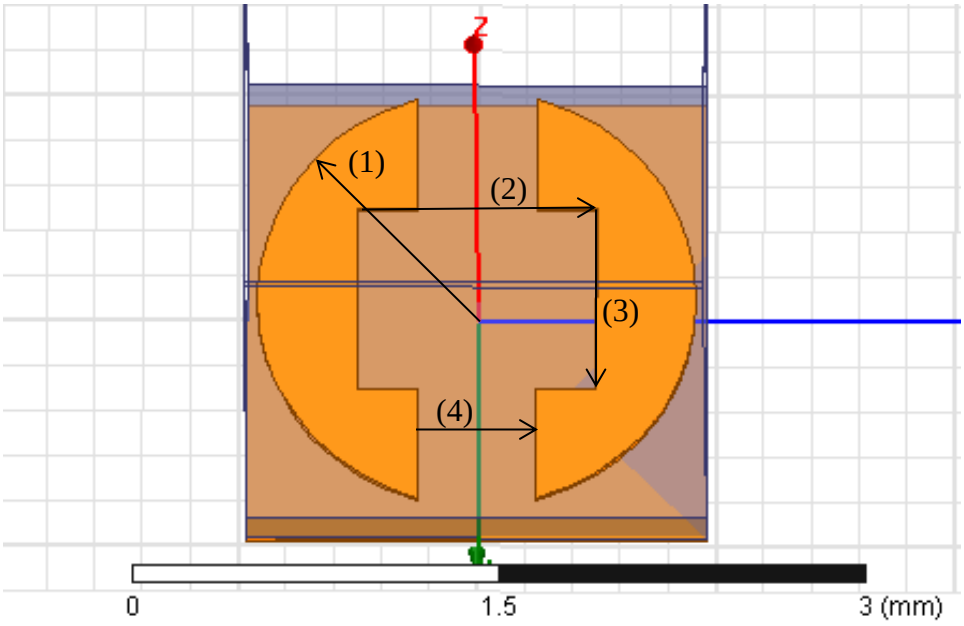

Figure 3: Image of 0° zone patch. The dimensions are defined as (1) CuRad, (2) w2, (3) h2, and (4) w.

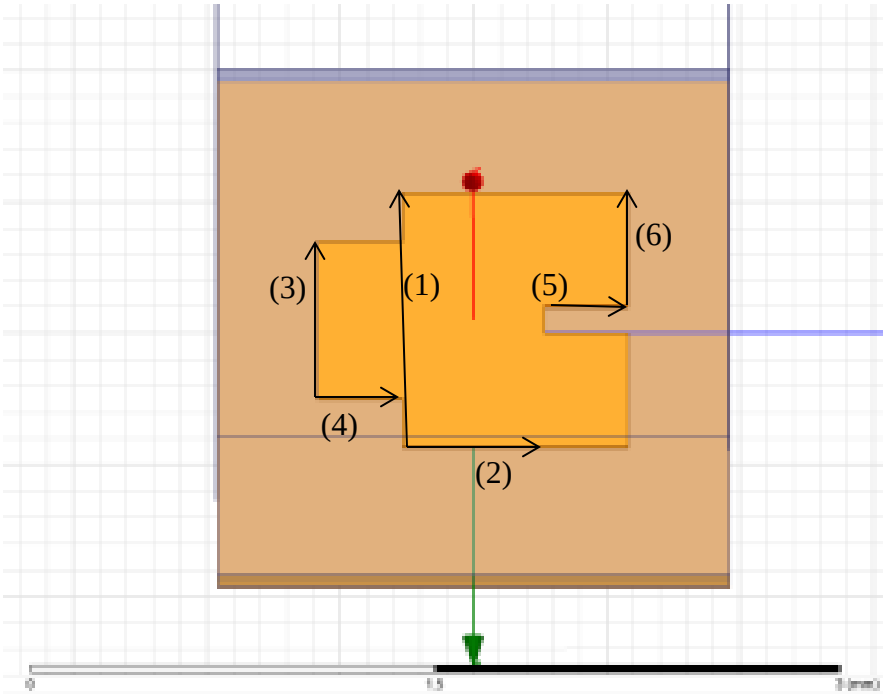

Figure 4: Image of 45° zone patch. The dimensions are defined as (1) x1, (2) y1, (3) x2, (4) y2, (5) x3, (6) y3. The two smaller rectangles on the right side of the patch both have the same dimensions.

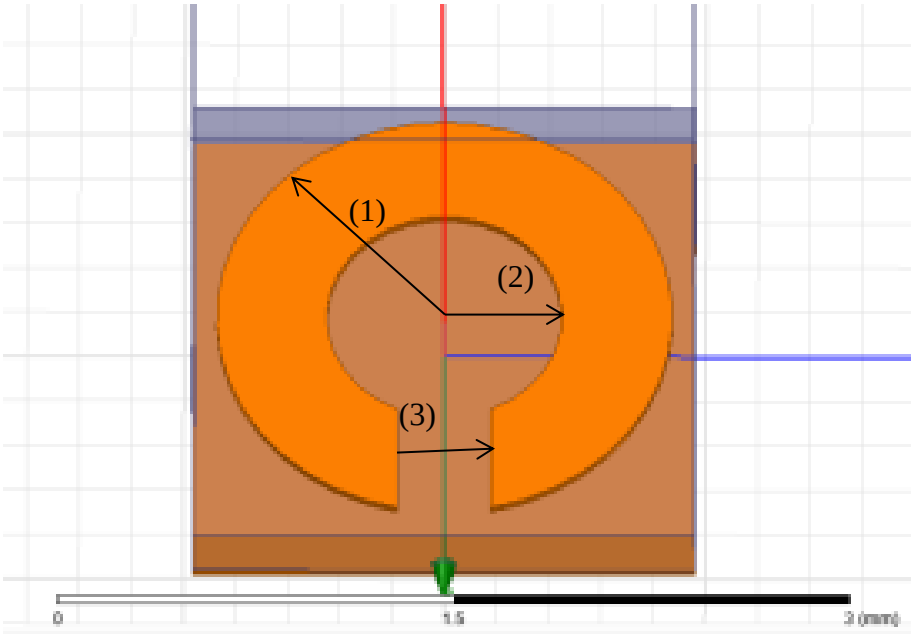

Figure 5: Image of 90° zone patch. The dimensions are (1) r_ext, (2) r_in, and (3) height.

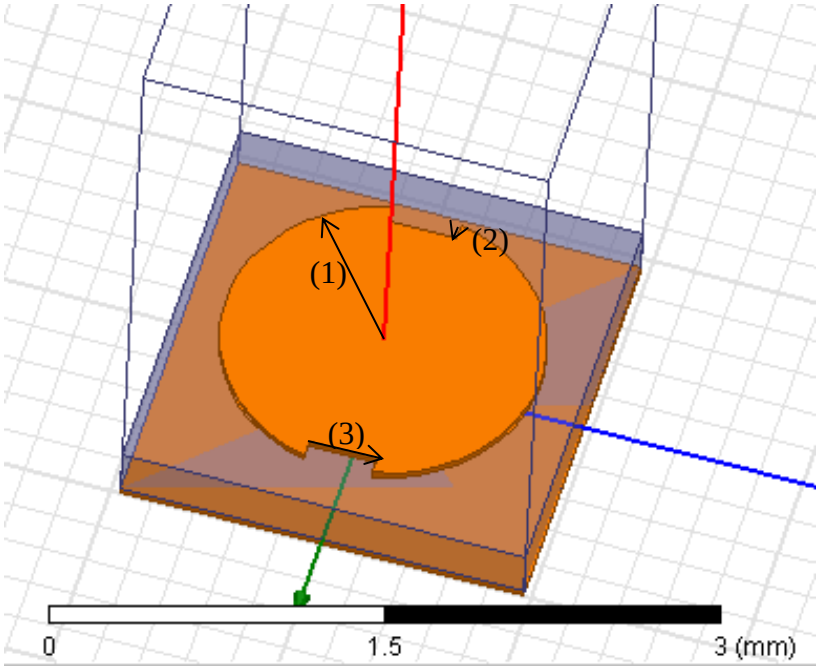

Figure 6: Image of 135° zone patch. The dimensions are defined as (1) Major Radius, (2) Delta Y, and (3) Delta X

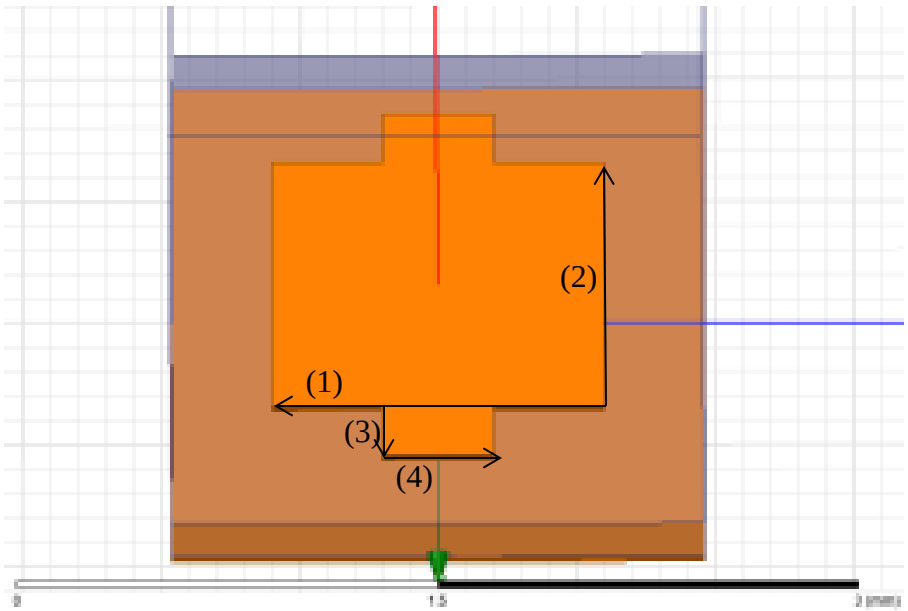

Figure 7: Image of 180° zone patch. The dimensions are defined as (1) ymain, (2) xmain, (3) xlittle, and (4) ylittle. The small rectangles on the top and bottom are identical.

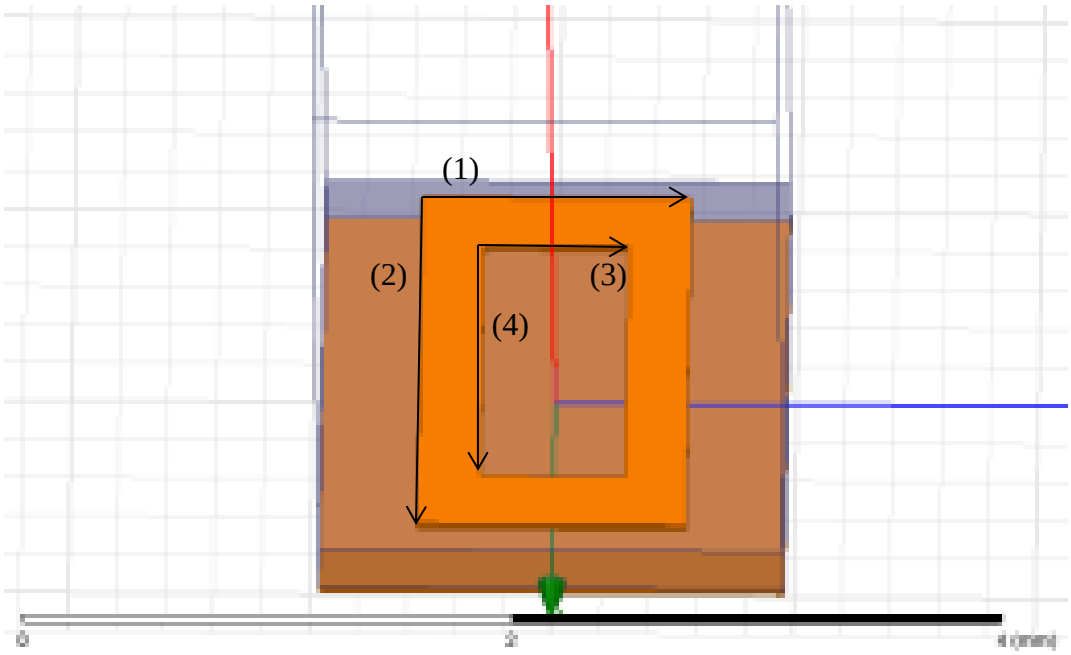

Figure 8: Image of the 225° zone patch. The dimensions are defined as (1) r_ext_y, (2) r_ext_x, (3) r_in_y, and (4) r_in_x.

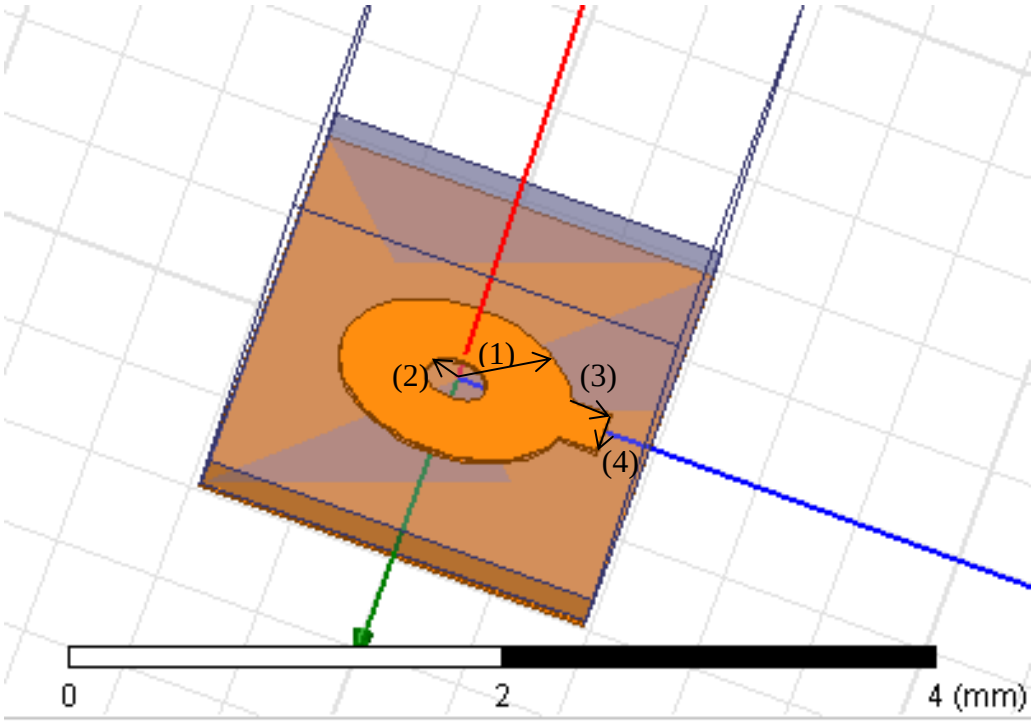

Figure 9: Image of the 270° zone patch. The dimensions are defined as (1) MajRad, (2) RTh, (3) w, and (4) l. There was also the axial ratio of the ellipses, defined as Ratio.

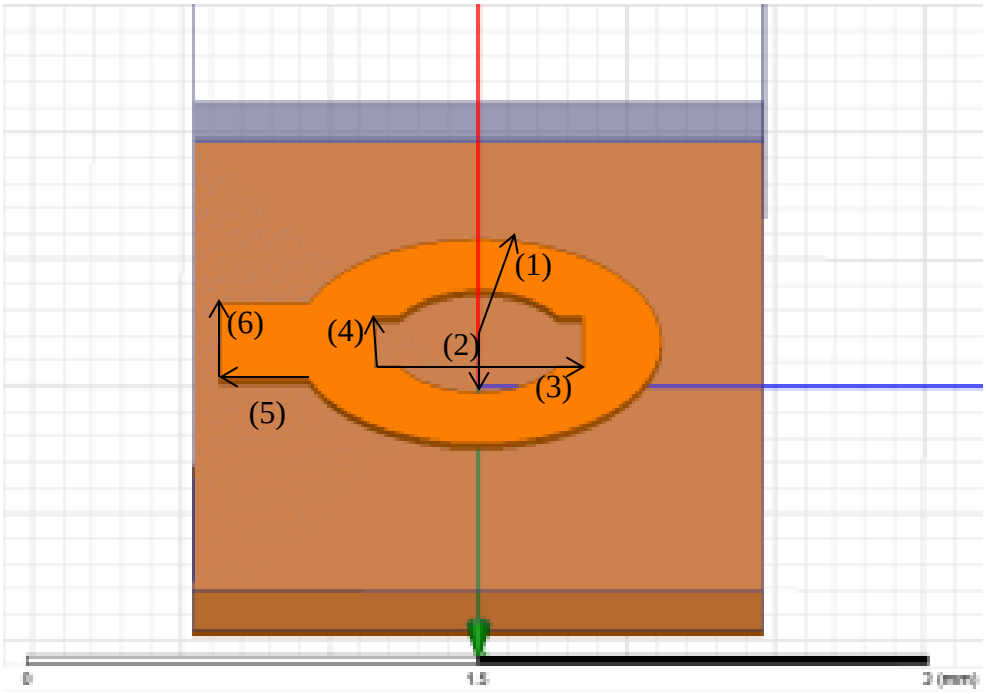

Figure 10: Image of the 315° zone patch. The dimensions are defined as (1) MajRad, (2) RadInt, (3) Ywidth, (4) Xwidth, (5) l, and (6) w. The ellipses also have an axial ratio called Ratio.

Once the y-polarizations were obtained, the x-polarizations needed to be measured and then possibly changed slightly to fit the required 90° phase difference for circular polarization. A similar sweep of the geometric variables was done to see if any of the variables changed the x-polarization but not the y-polarization. If a variable was found to tweak exclusively the x-polarization and not the y, it was changed to fit the 90° phase difference. If there were no variables found to affect exclusively the x-polarization, then the variables were slowly changed by hand in an attempt to align the phase reflections appropriately.

Once the changes were made, the measurements presented in the paper to characterize the patches were obtained. Since the axial ratio was defined in the paper as the ratio between the

maximum and minimum reflected field, the maximum and the minimum of the reflected field were obtained. The ΔΦº was defined as the difference in the reflected y-phase and x-phase.

3. Results and Conclusions

This chapter is broken into two parts. The first, Results and Discussion, presents the results and attempts to explain the differences in results. The second section, Conclusions, summarizes the report.

D. Results and Discussion

The geometric sweep results can be seen in Figure 11 through Figure 46. These sweeps were intended as a guide to show which dimensions to manipulate to obtain the desired reflection phase. For example, the 0° zone patch was seen to respond well to changing the dimension CuRad, but not change significantly when changing w, h2, or w2. This meant that the optimization of the patch was done using just CuRad.

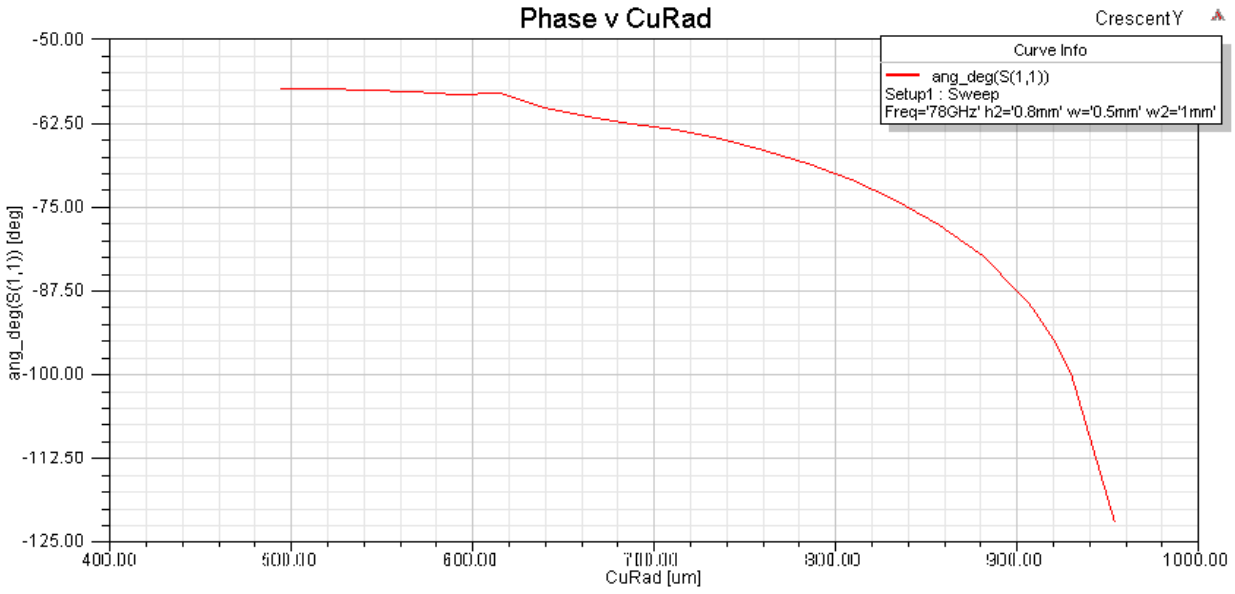

Figure 11: Sweep of CuRad for the 0° zone patch

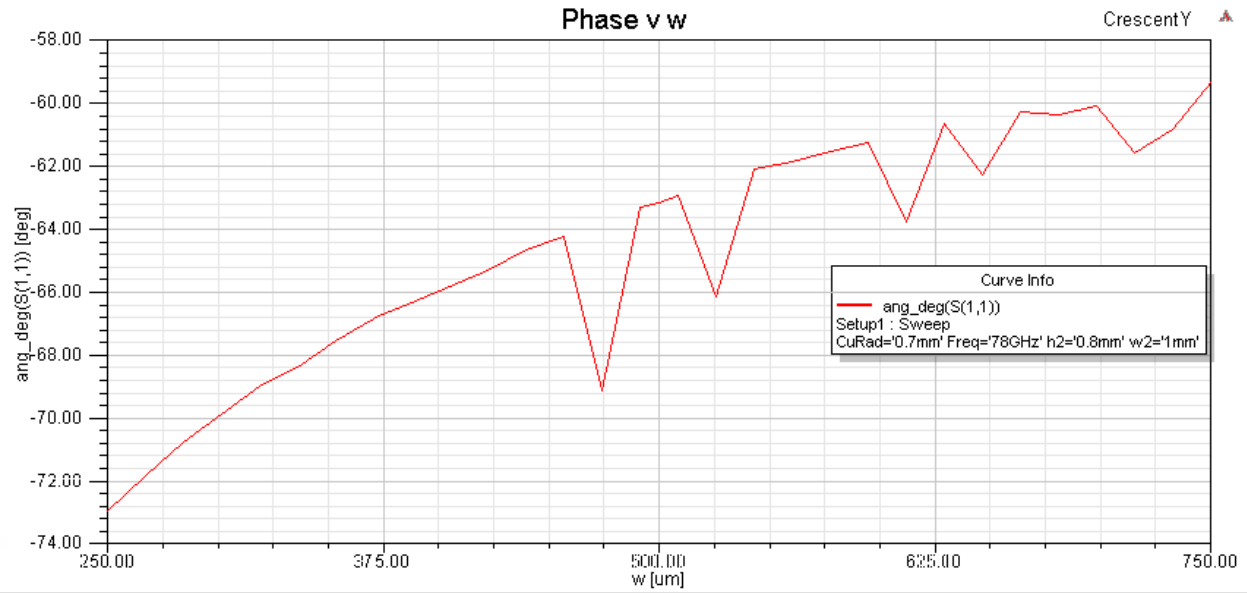

Figure 12: Sweep of w for the 0° zone patch

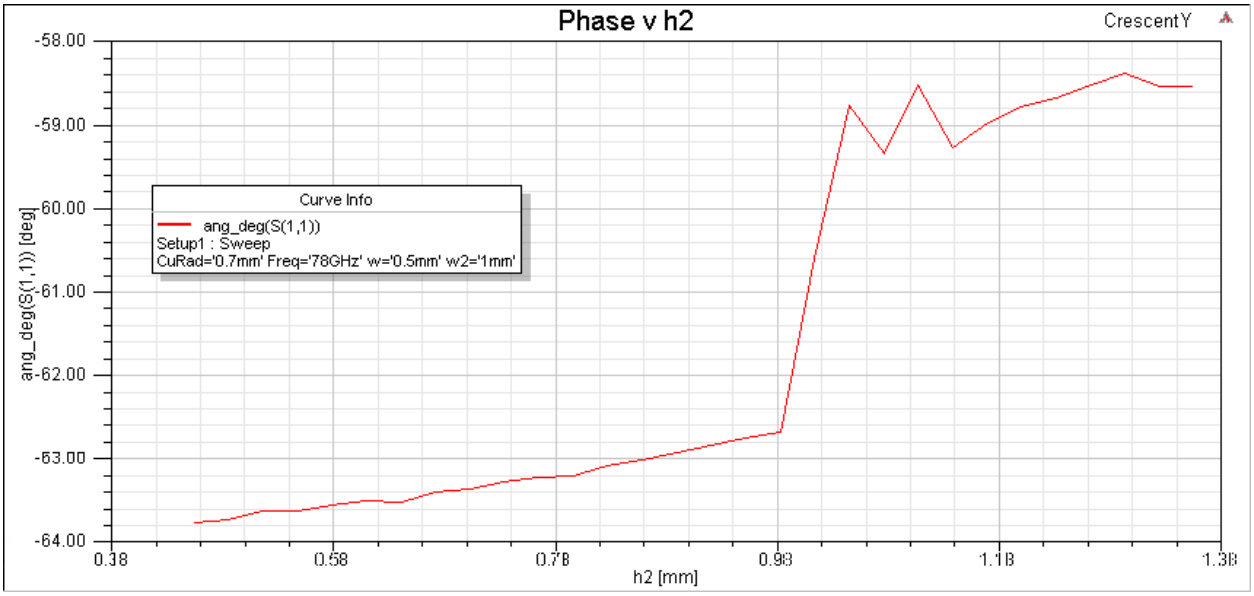

Figure 13: Sweep of h2 for the 0° zone patch

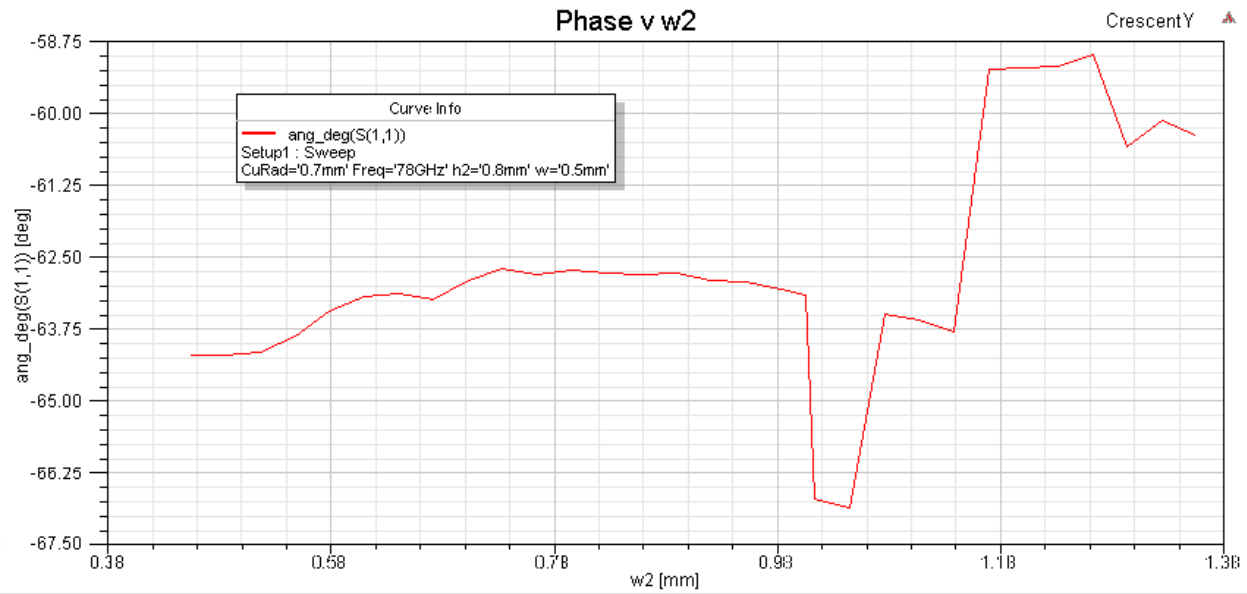

Figure 14: Sweep of w for the 0° zone patch

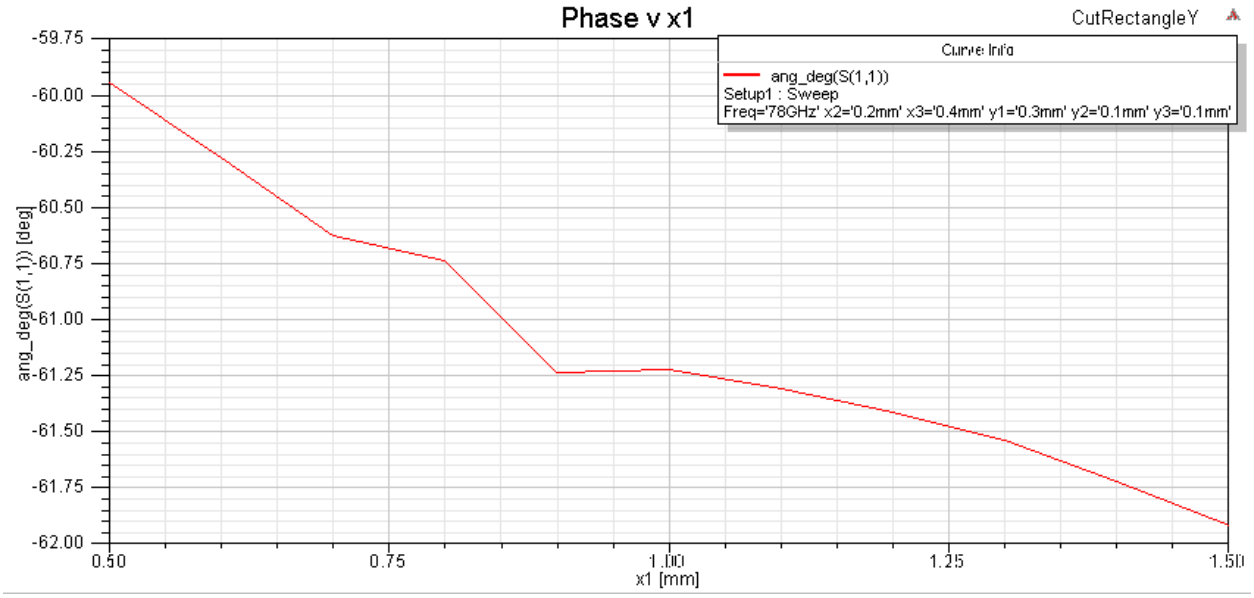

Figure 15: Sweep of x1 for the 45° zone patch

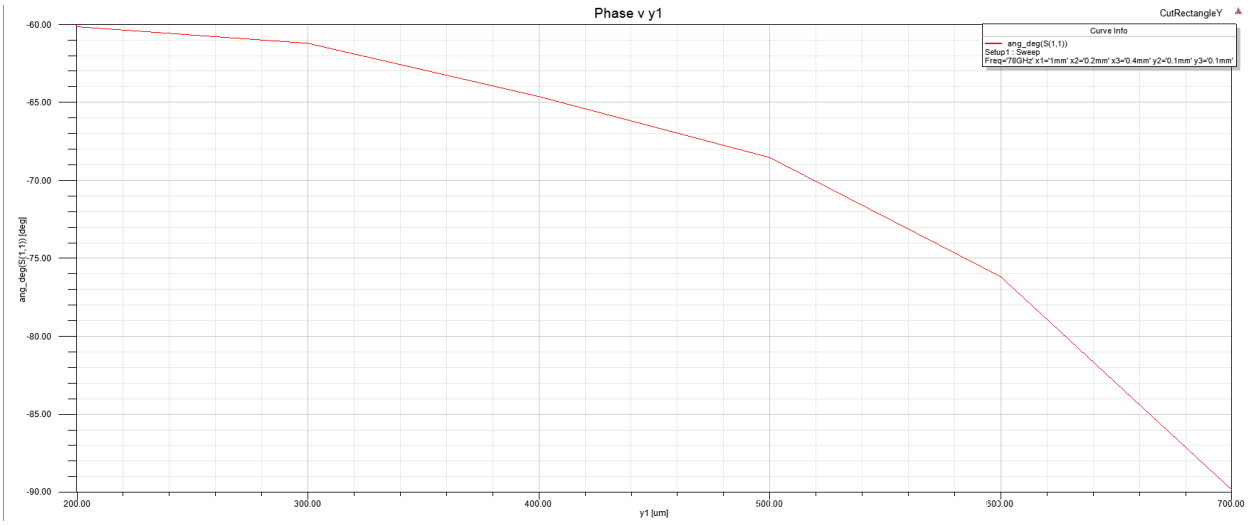

Figure 16: Sweep of y1 for the 45° zone patch

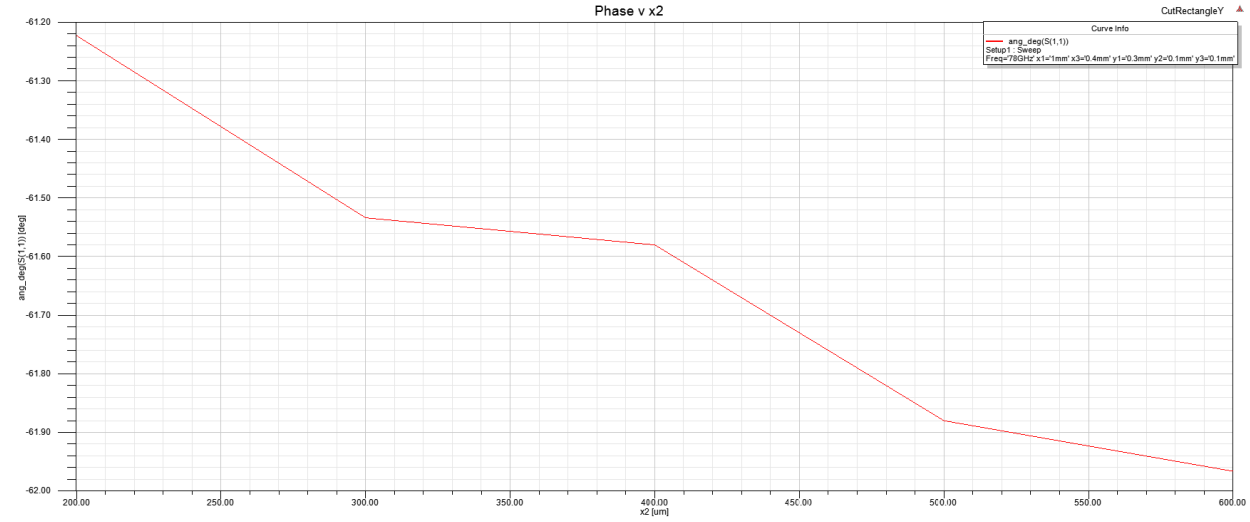

Figure 17: Sweep of x2 for the 45° zone patch

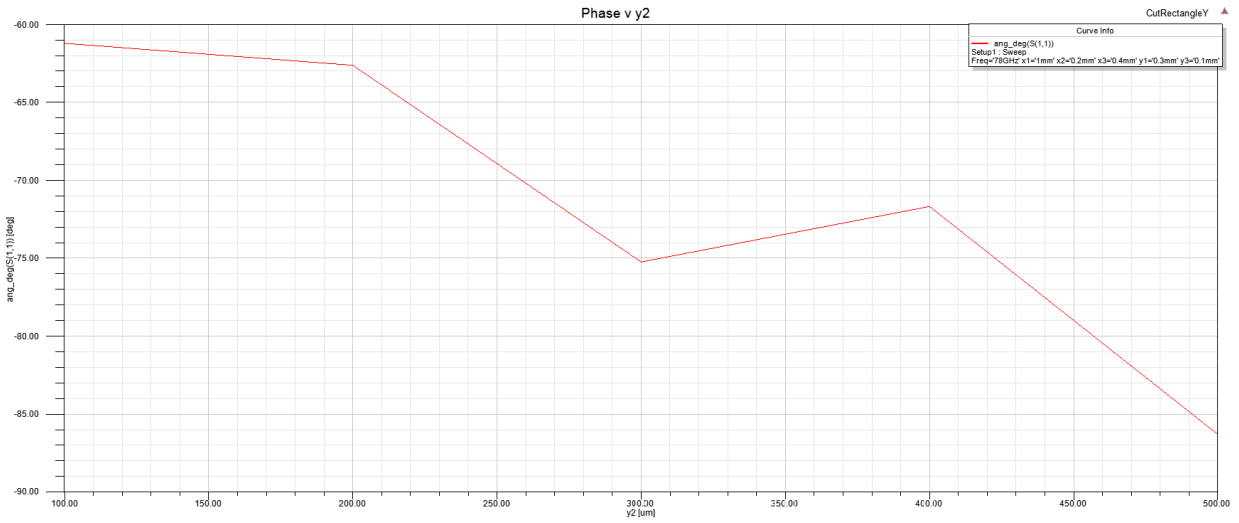

Figure 18: Sweep of y2 for the 45° zone patch

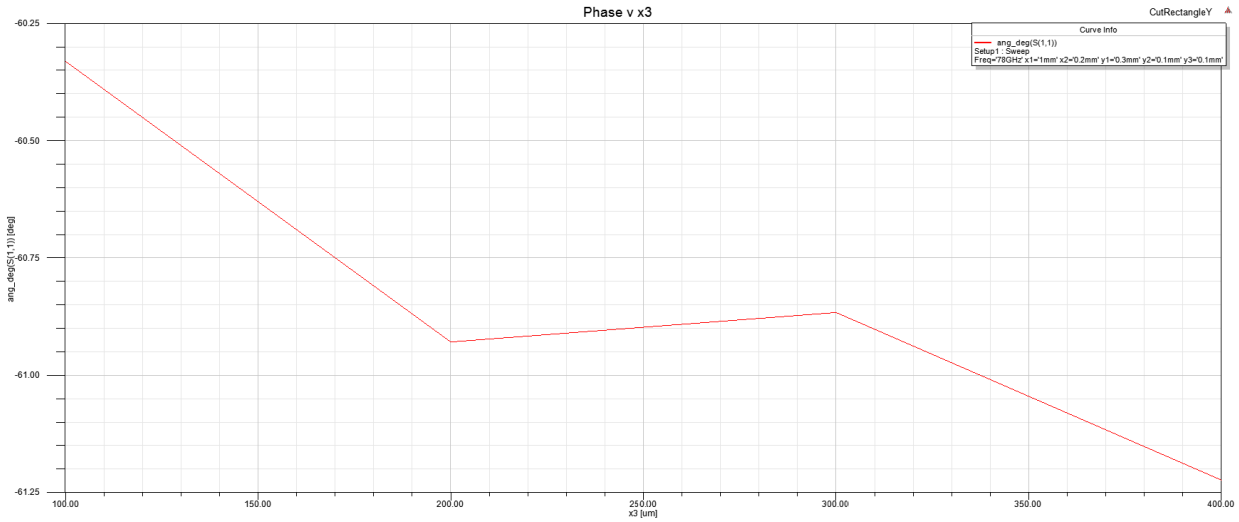

Figure 19: Sweep of x3 for the 45° zone patch

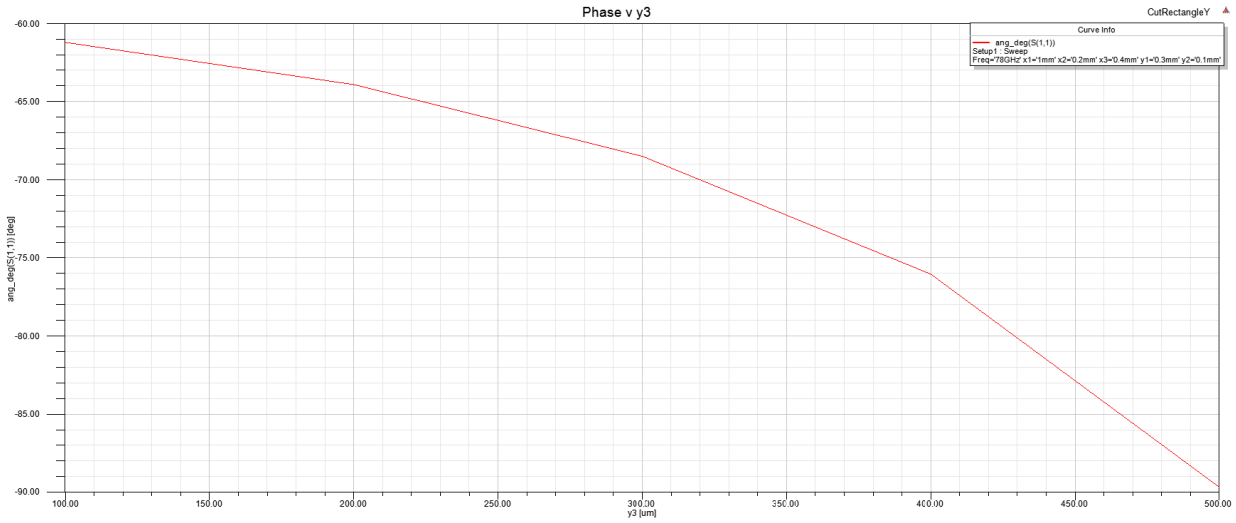

Figure 20: Sweep of y3 for the 45° zone patch

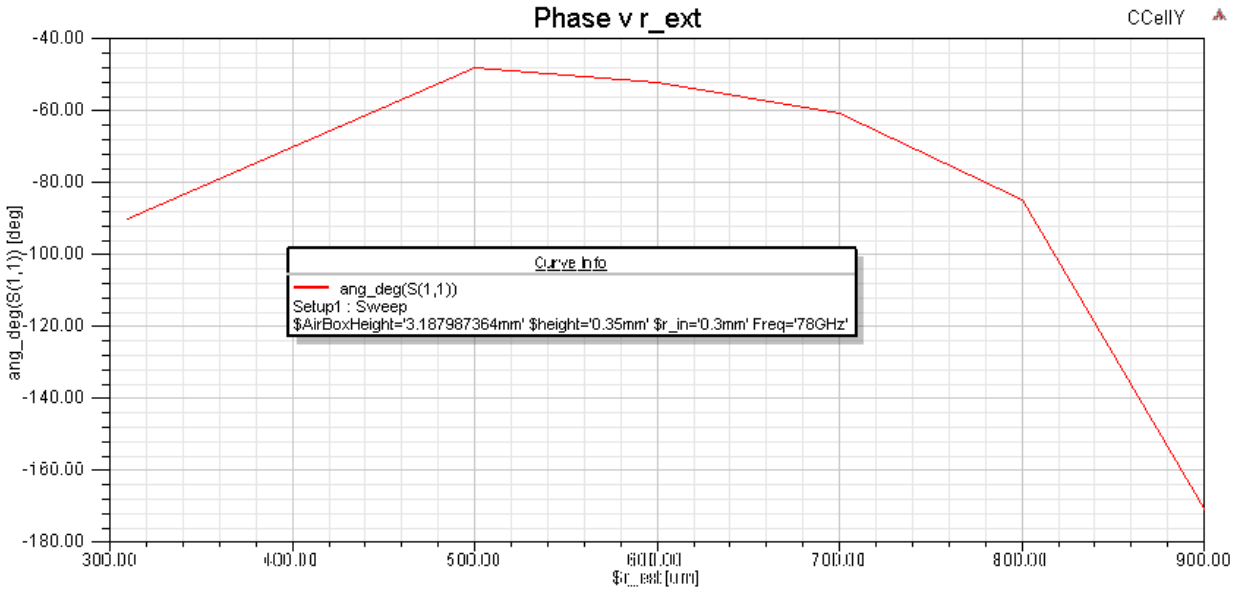

Figure 21: Sweep of r_ext for the 90° zone patch

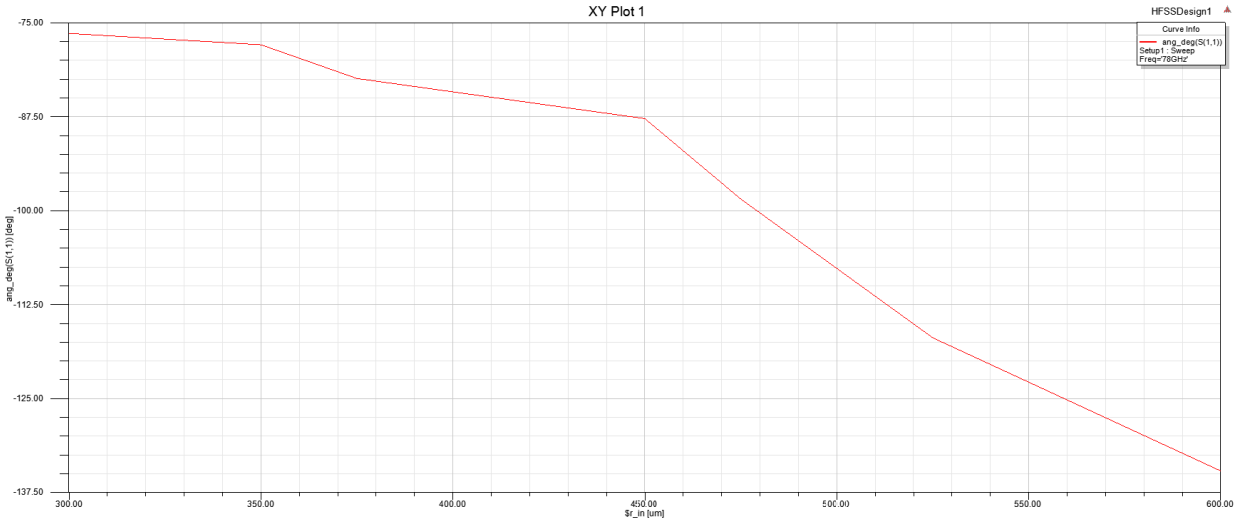

Figure 22: Sweep of r_in for the 90° zone patch

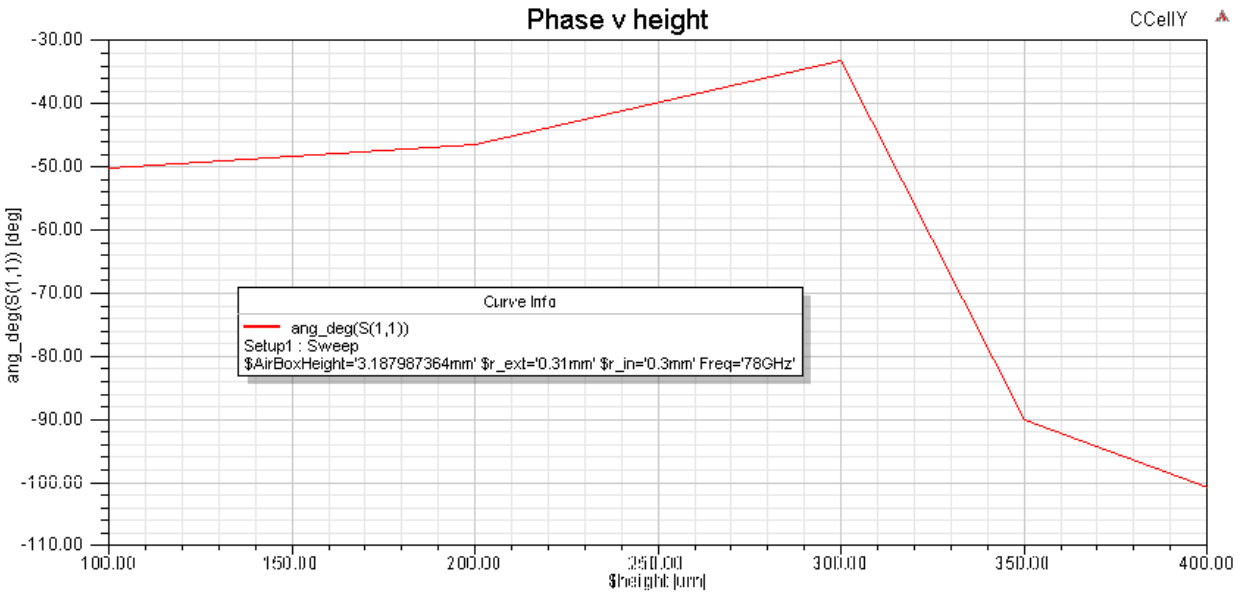

Figure 23: Sweep of height for the 90° zone patch

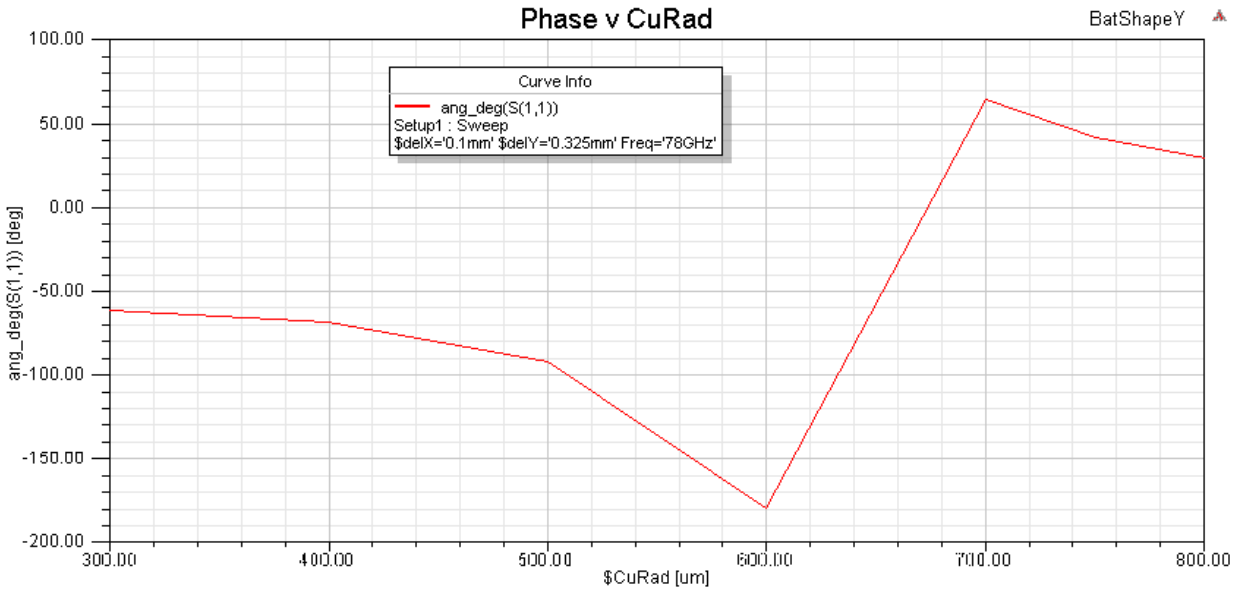

Figure 24: Sweep of CuRad for 135° zone patch

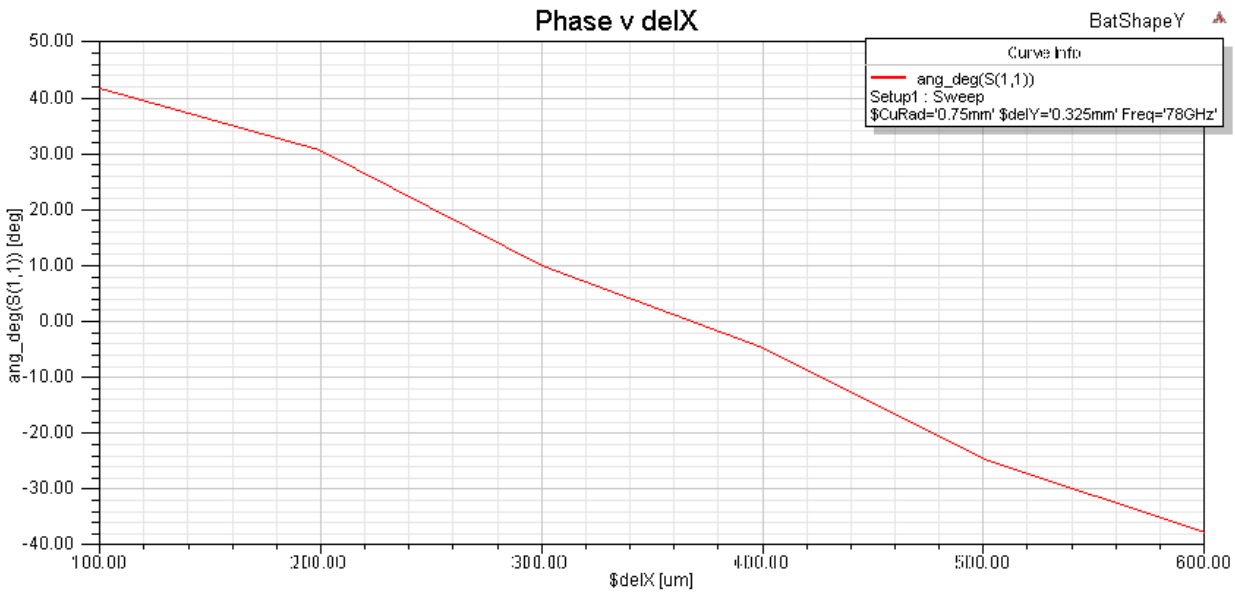

Figure 25: Sweep of delX for the 135° zone patch

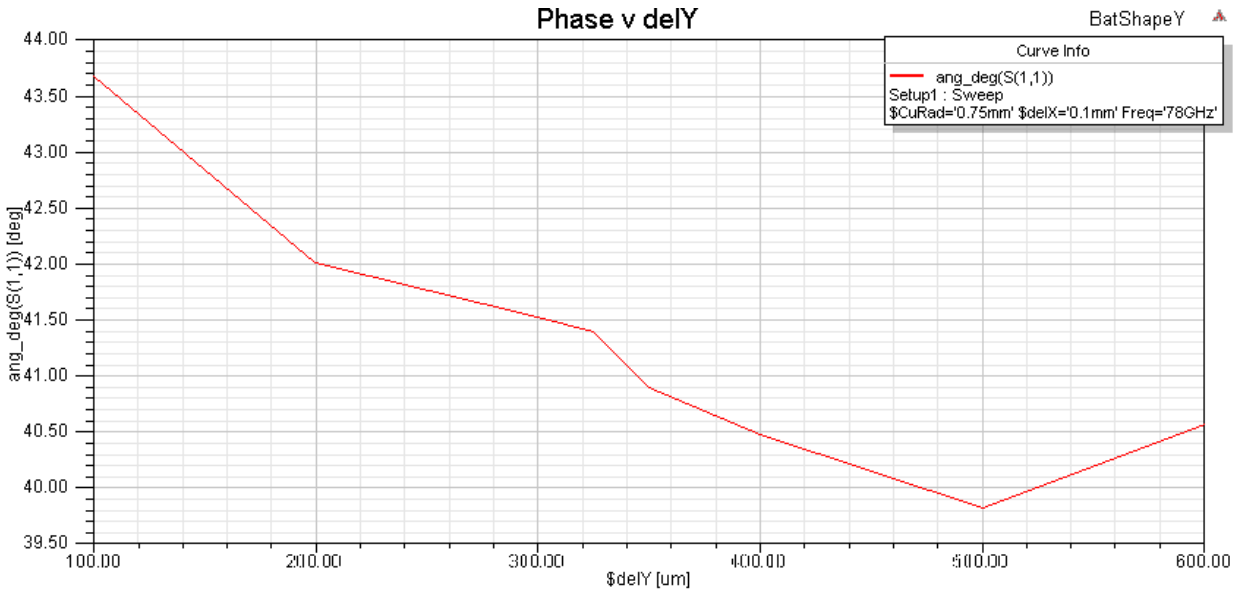

Figure 26: Sweep of delY for the 135° zone patch

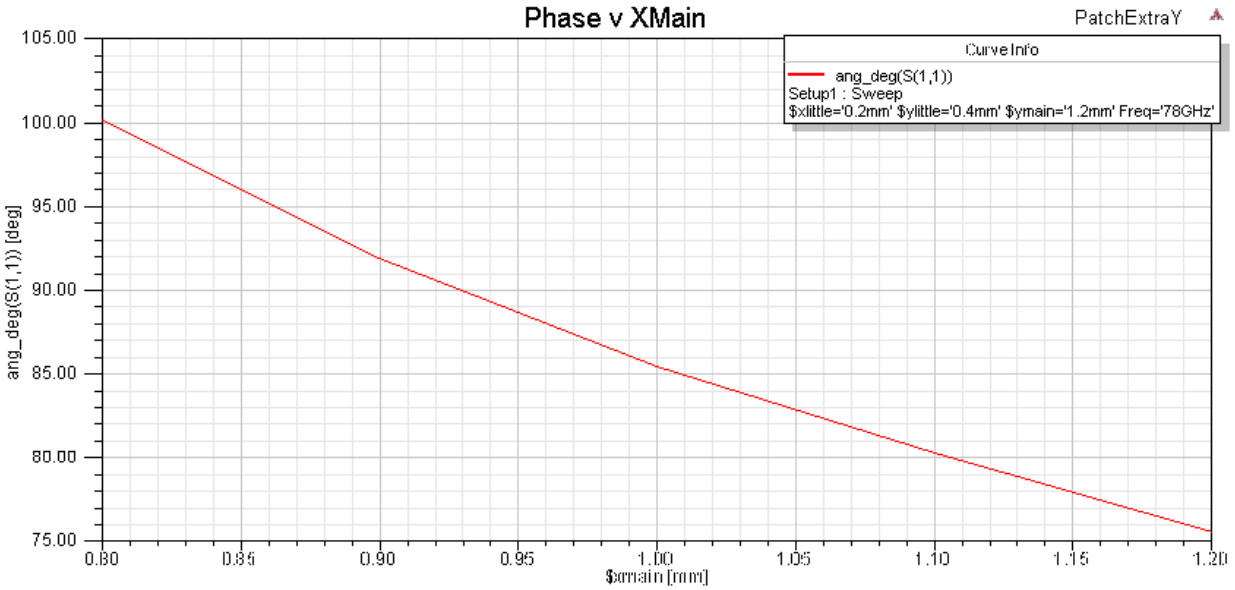

Figure 27: Sweep of Xmain for the 180° zone patch

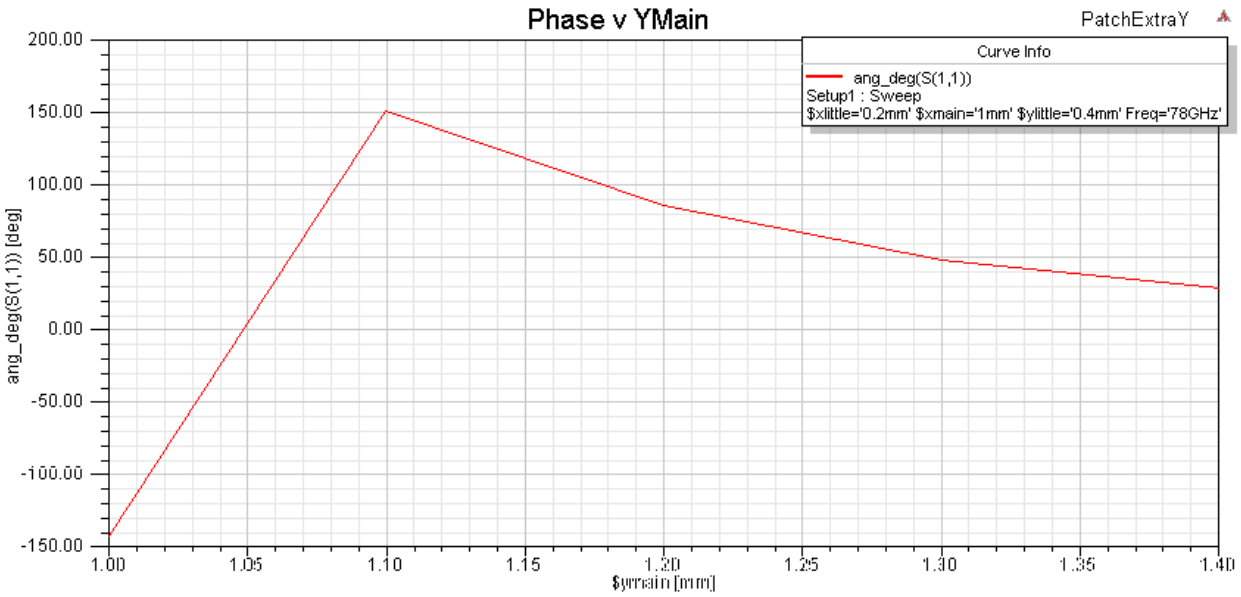

Figure 28: Sweep for Ymain for the 180° zone patch

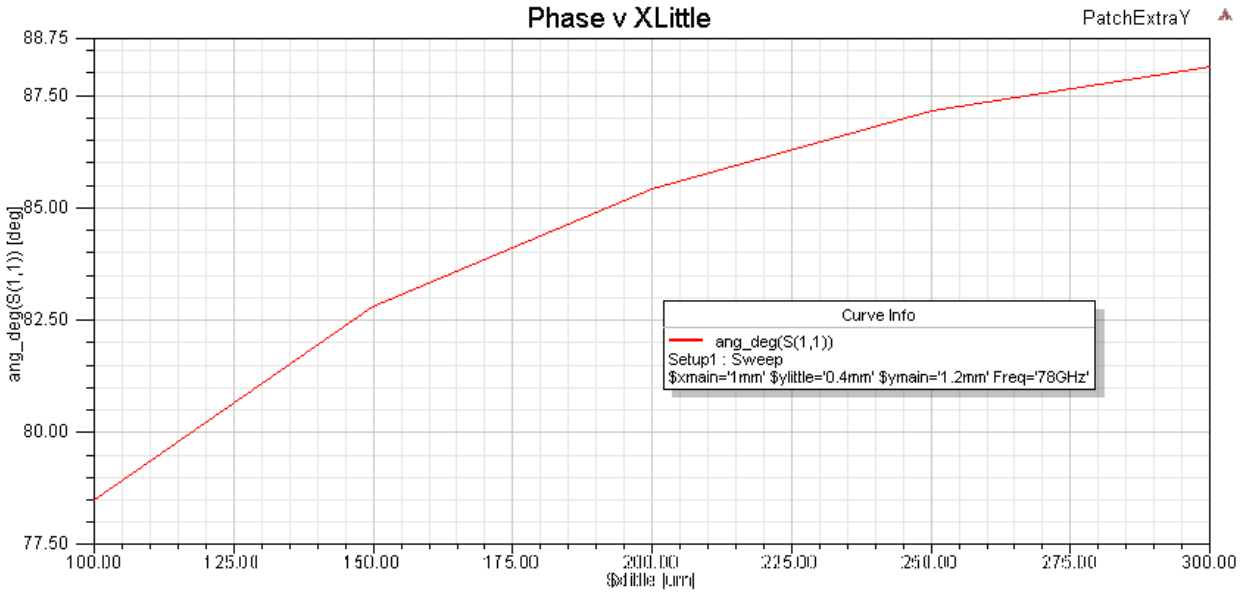

Figure 29: Sweep for XLittle for the 180° zone patch

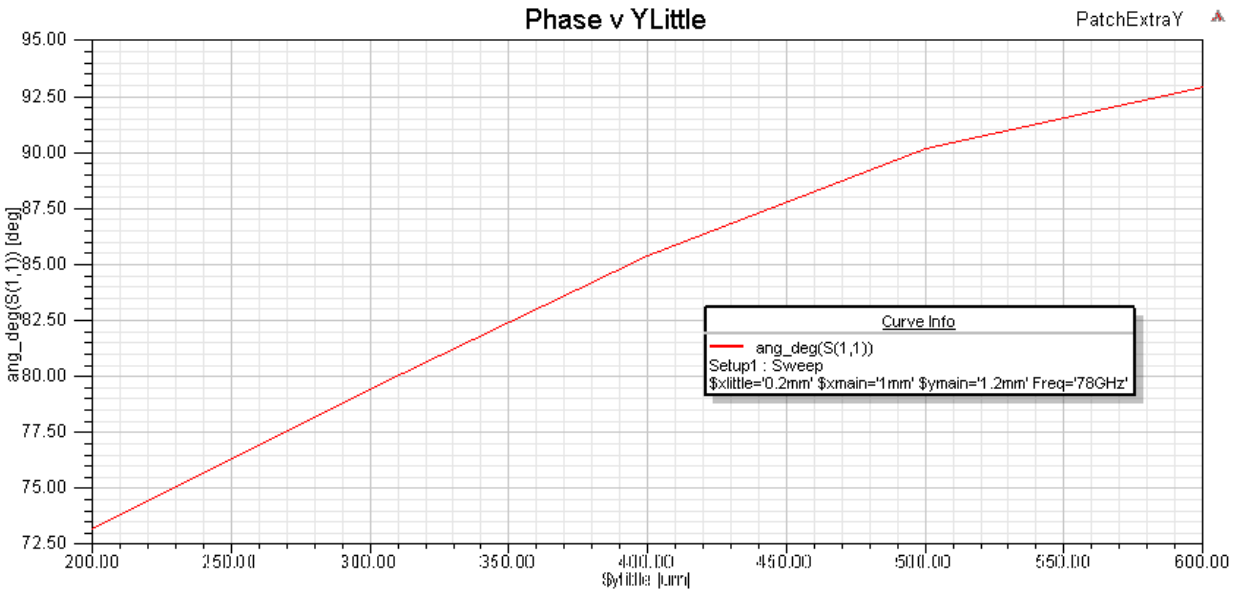

Figure 30: Sweep for YLittle for the 180° zone patch

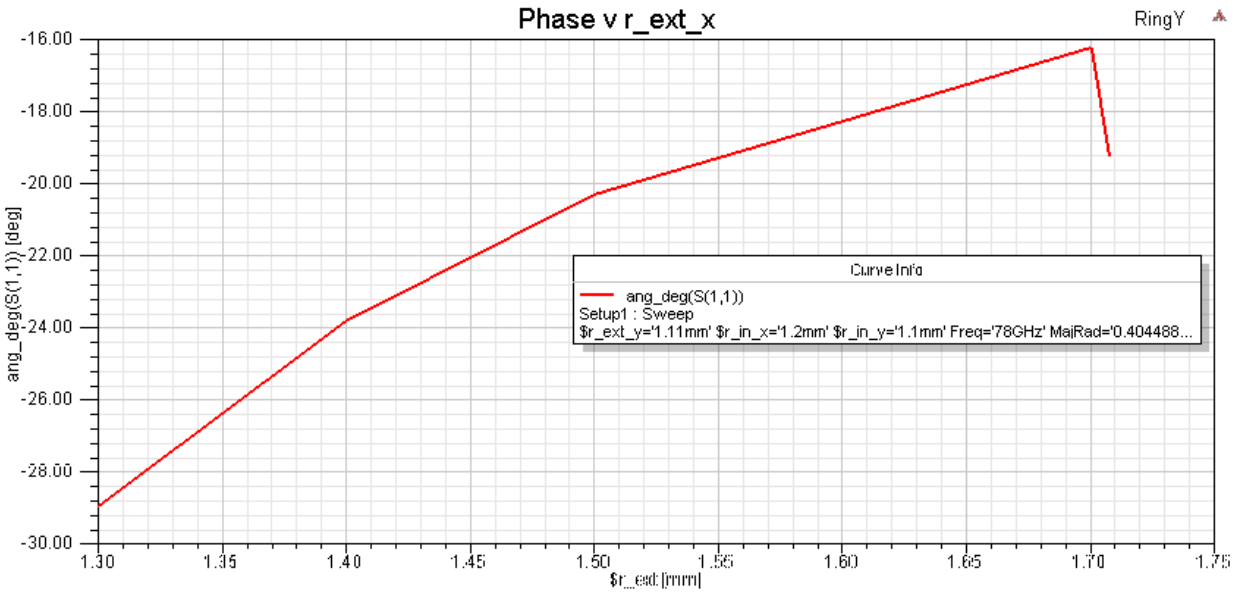

Figure 31: Sweep for r_ext_x for the 225° zone patch

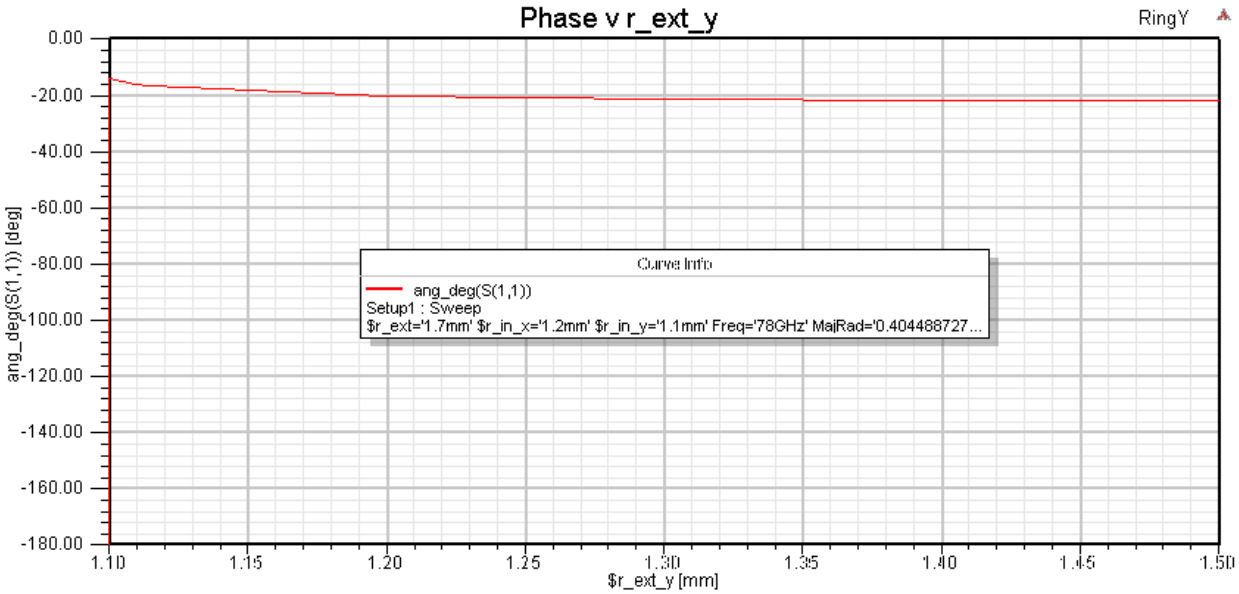

Figure 32: Sweep for r_ext_y for the 225° zone patch

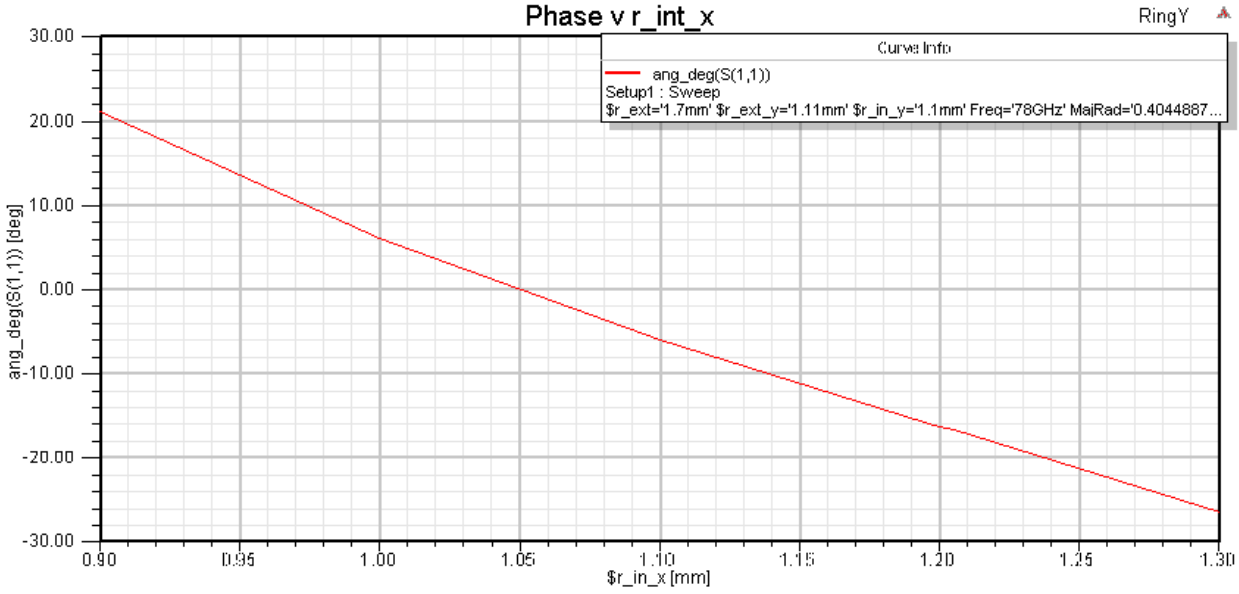

Figure 33: Sweep for r_in_x for the 225° zone patch

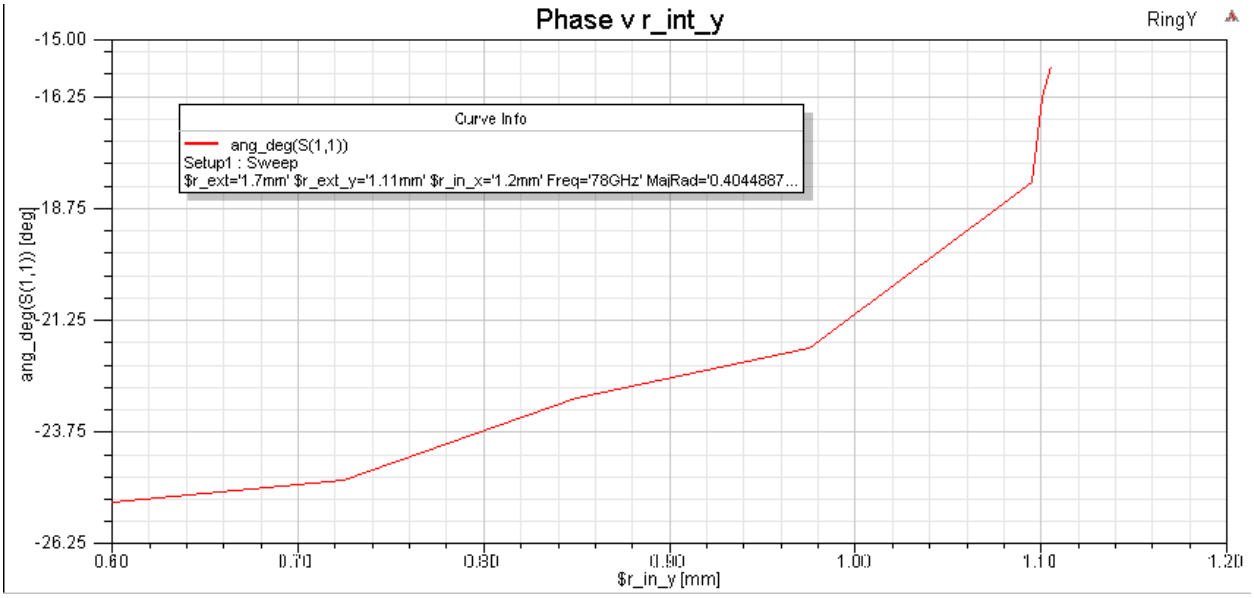

Figure 34: Sweep for r_in_y for the 225° zone patch

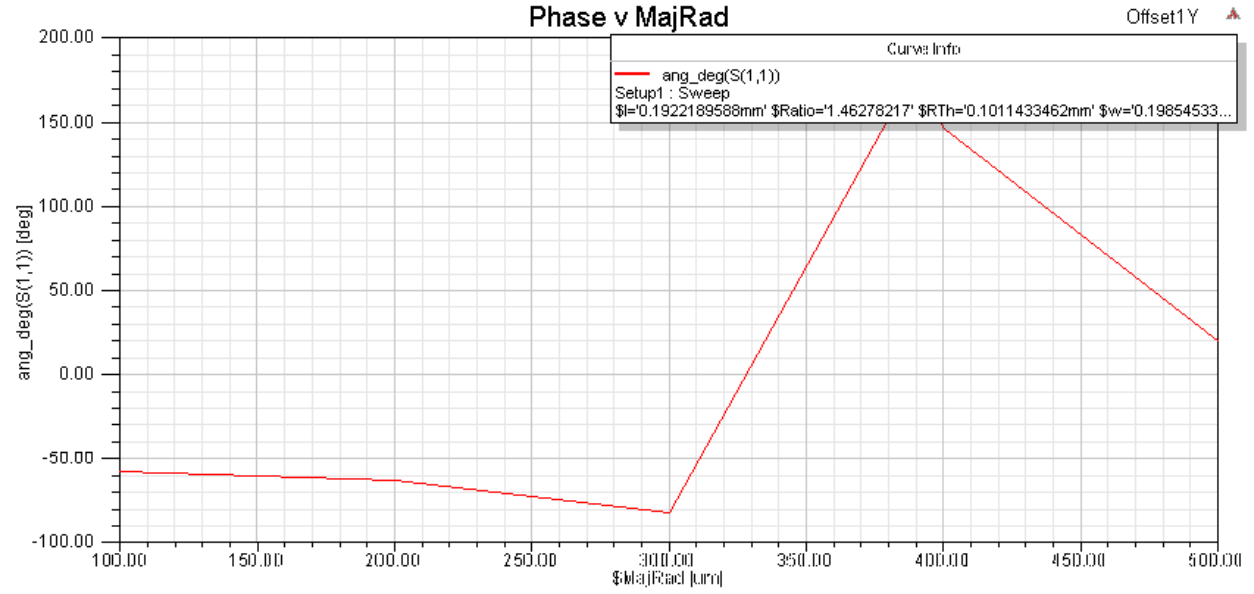

Figure 35: Sweep for MajRad for the 270° zone patch

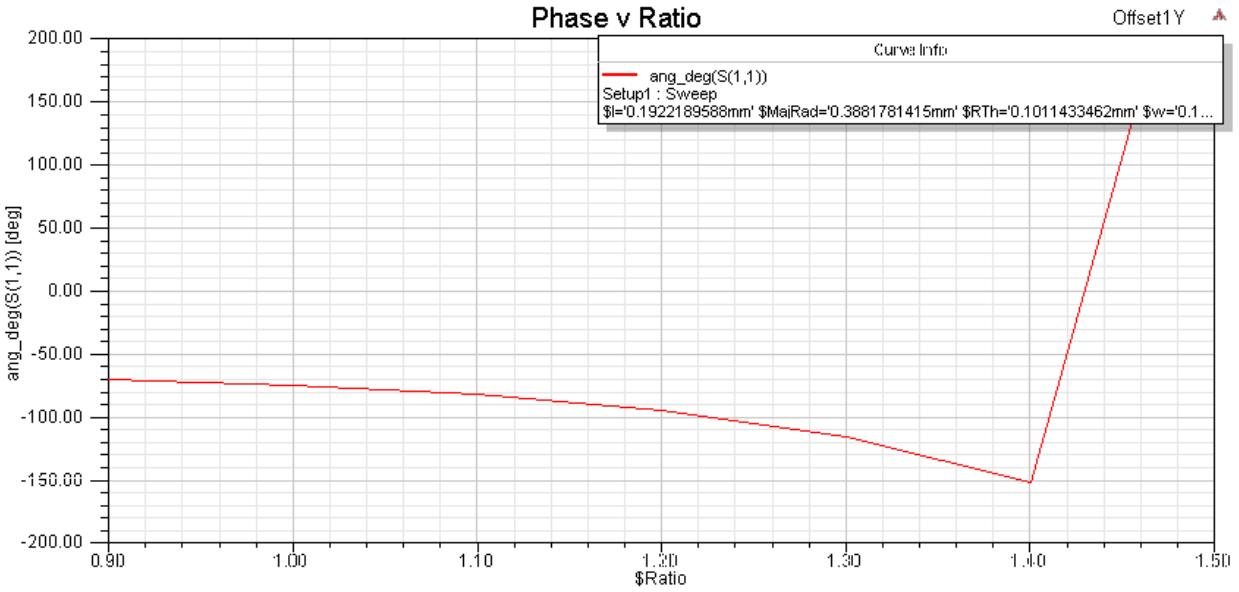

Figure 36: Sweep for Ratio for the 270° zone patch

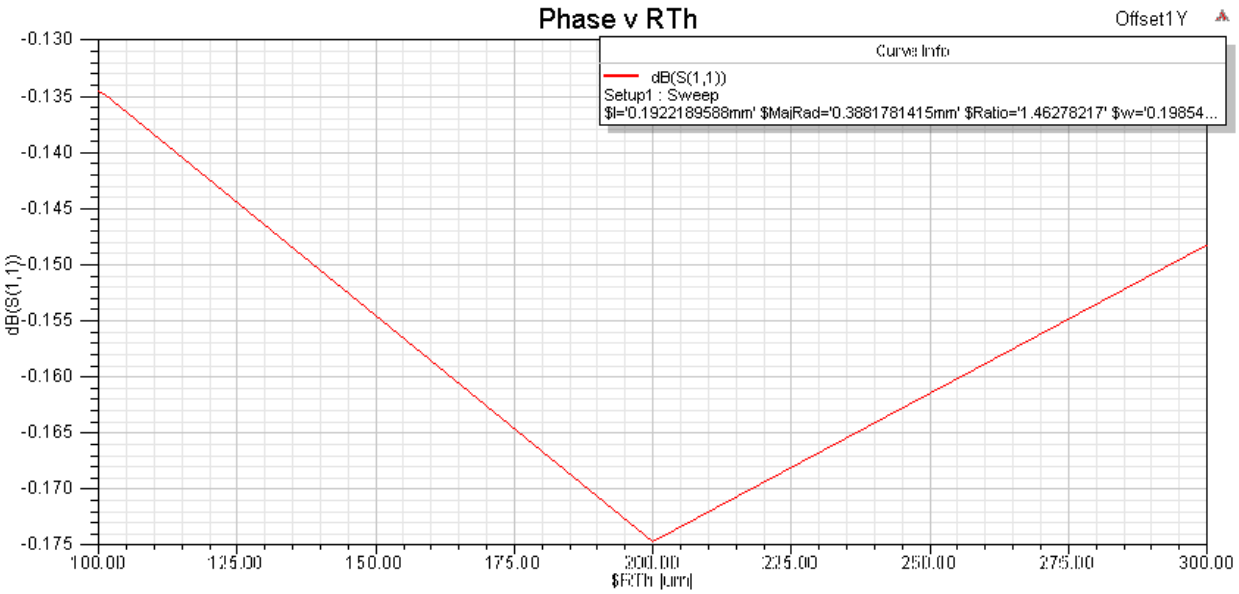

Figure 37: Sweep for RTh for the 270° zone patch

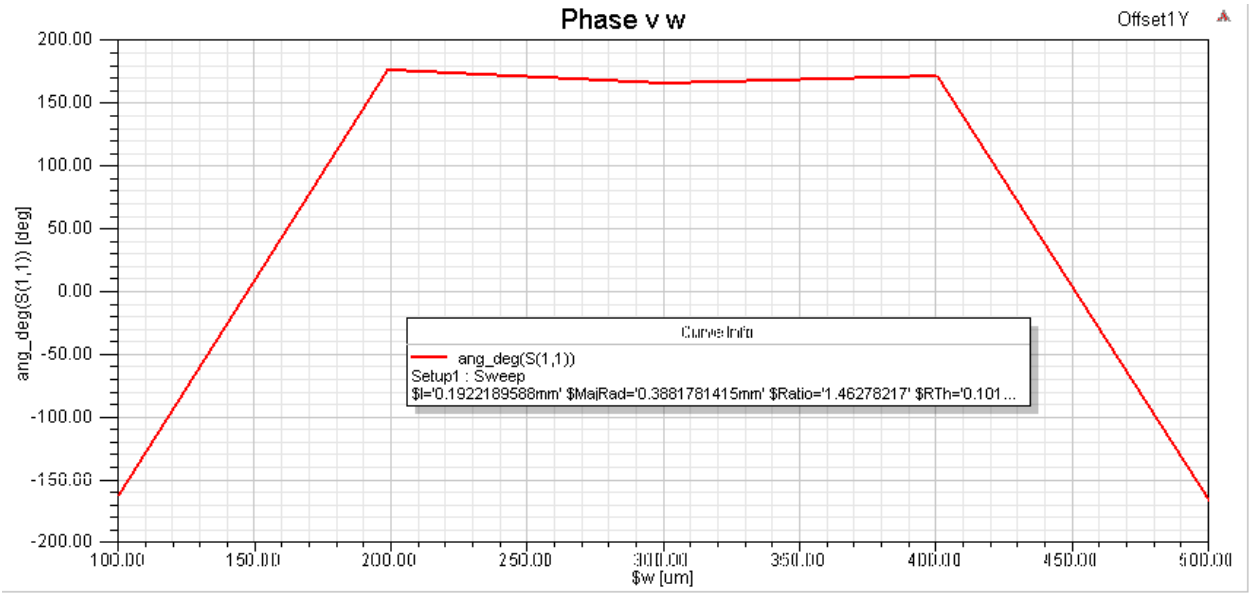

Figure 38: Sweep for w for the 270° zone patch

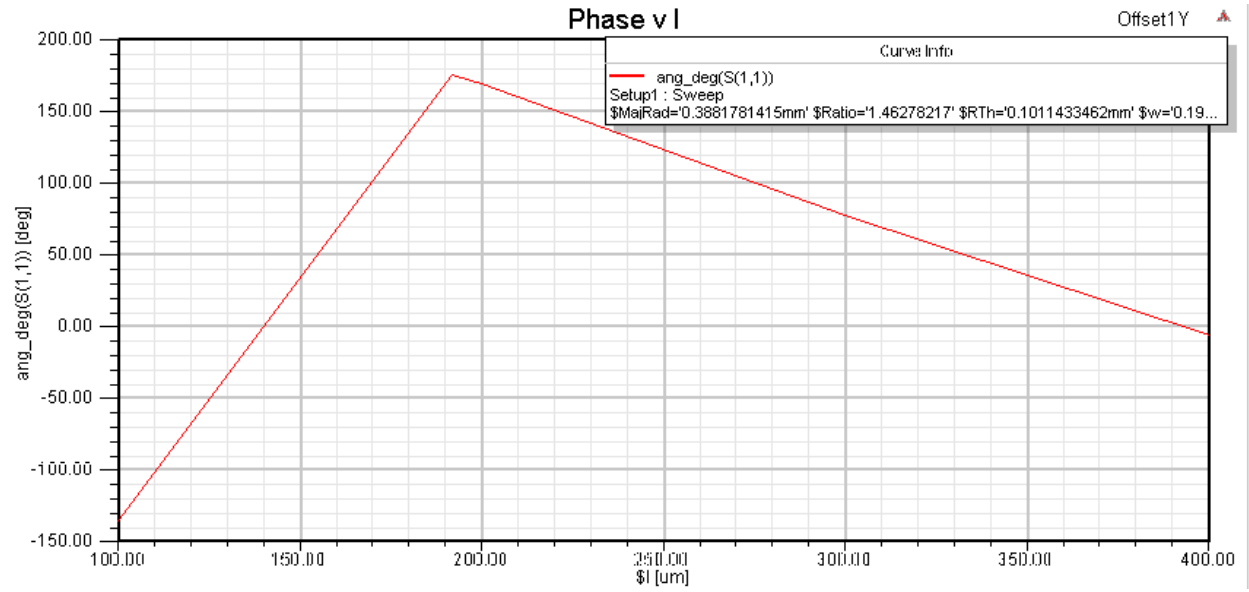

Figure 39: Sweep for l for the 270° patch

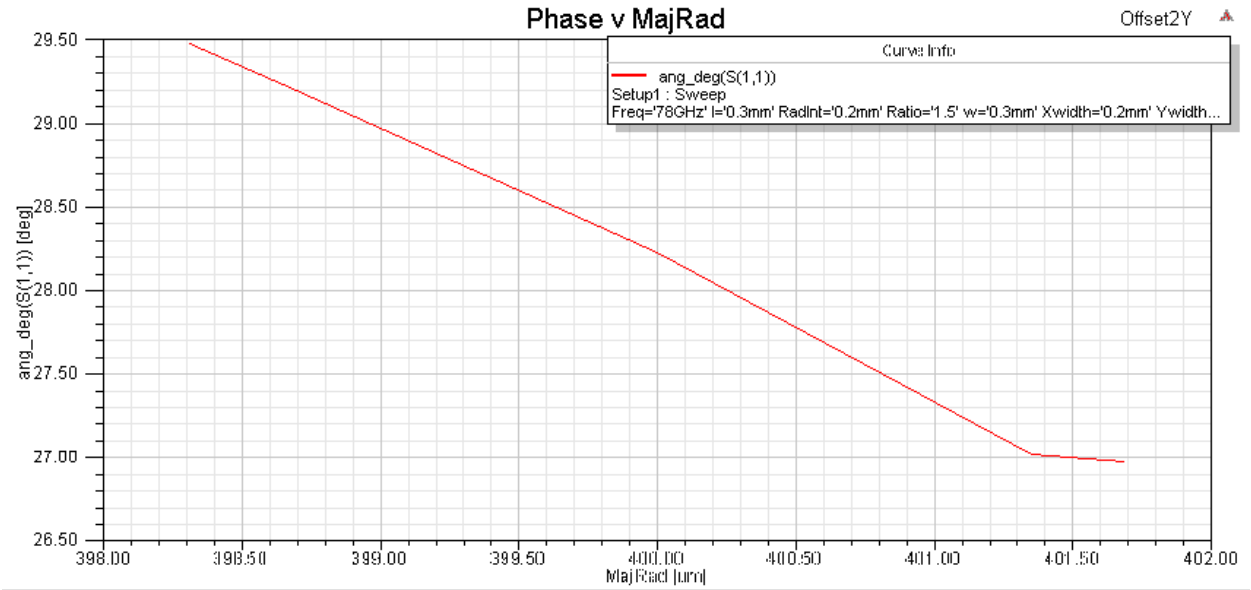

Figure 40: Sweep for MajRad for the 315° zone patch

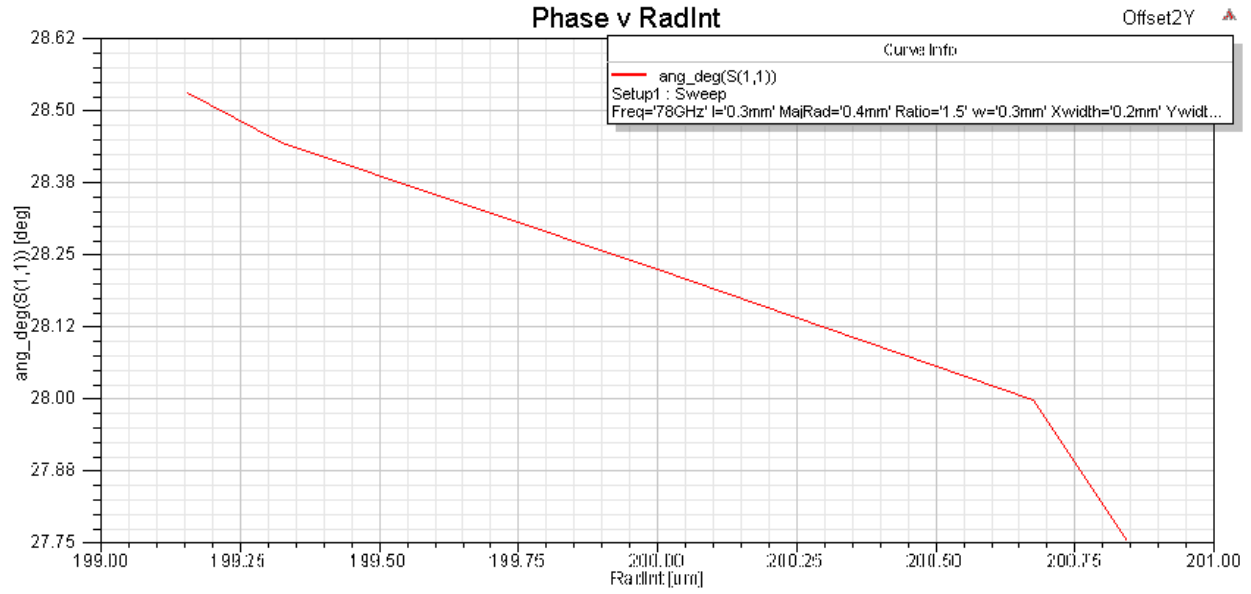

Figure 41: Sweep for RadInt for the 315° zone patch

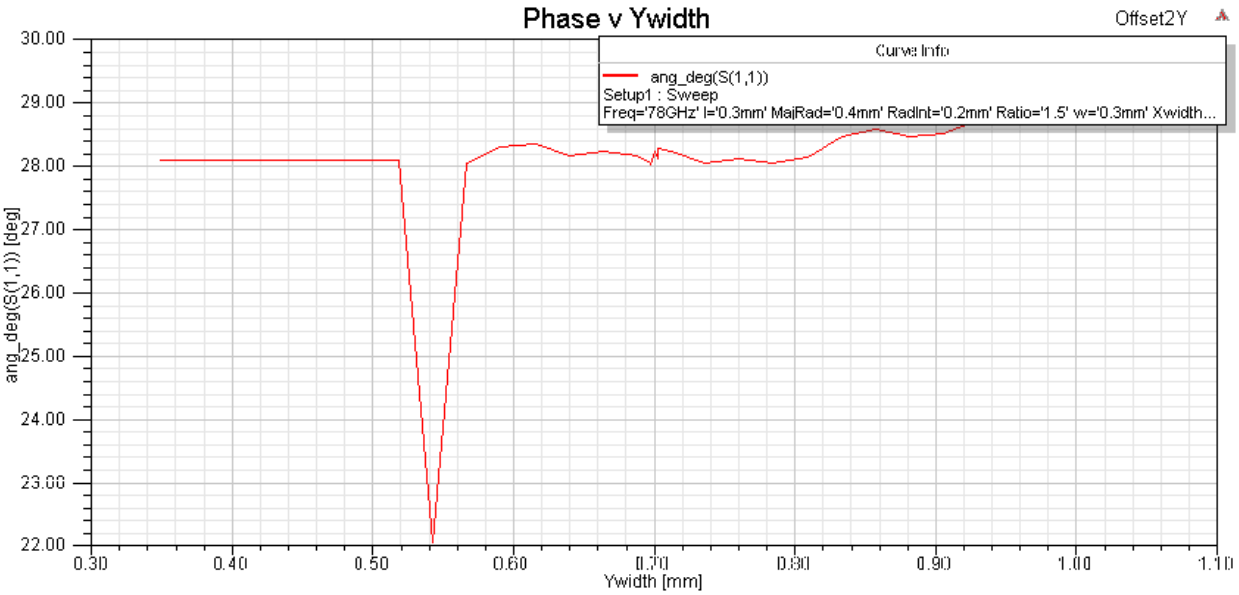

Figure 42: Sweep for Ywidth for the 315° zone patch

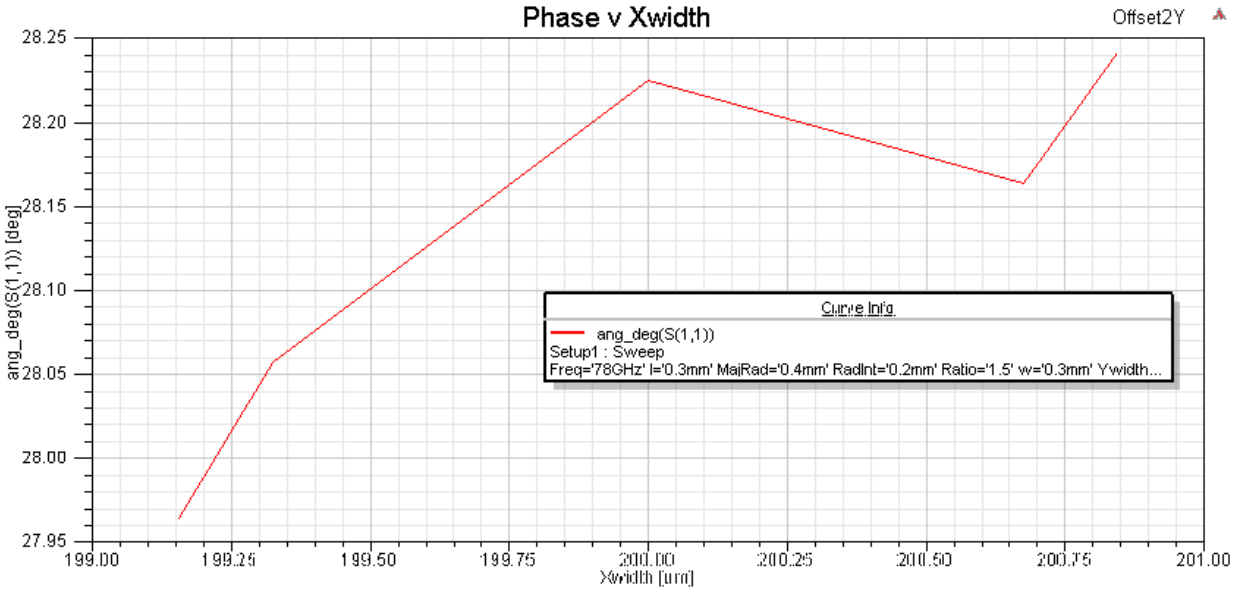

Figure 43: Sweep for Xwidth for the 315° zone patch

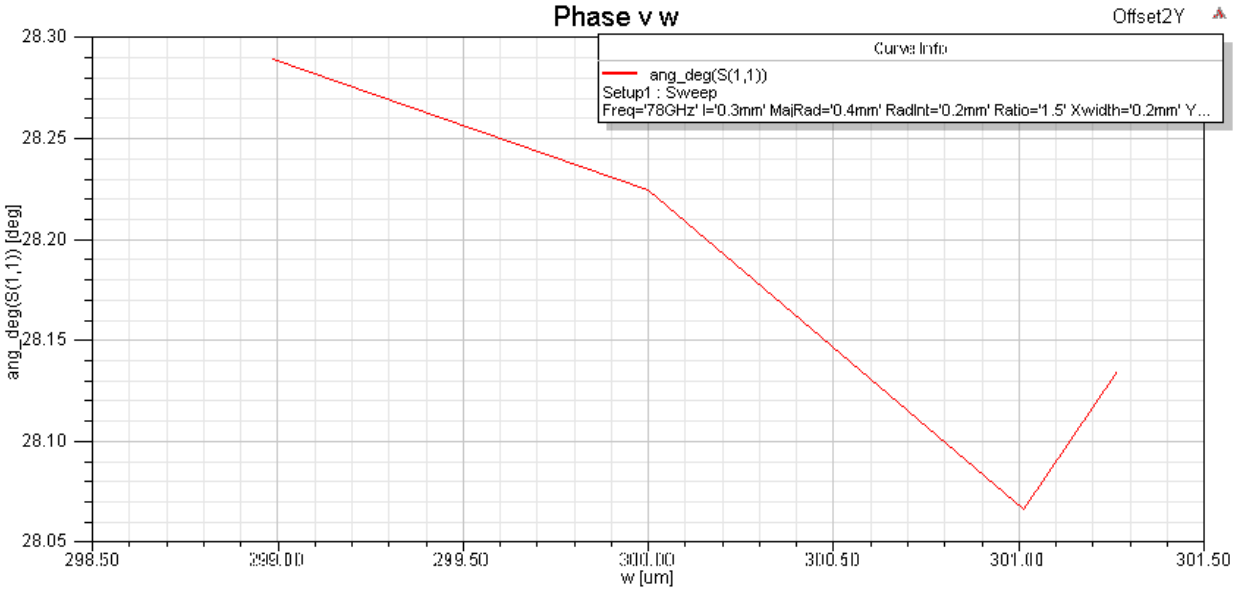

Figure 44: Sweep for w for the 315° zone patch

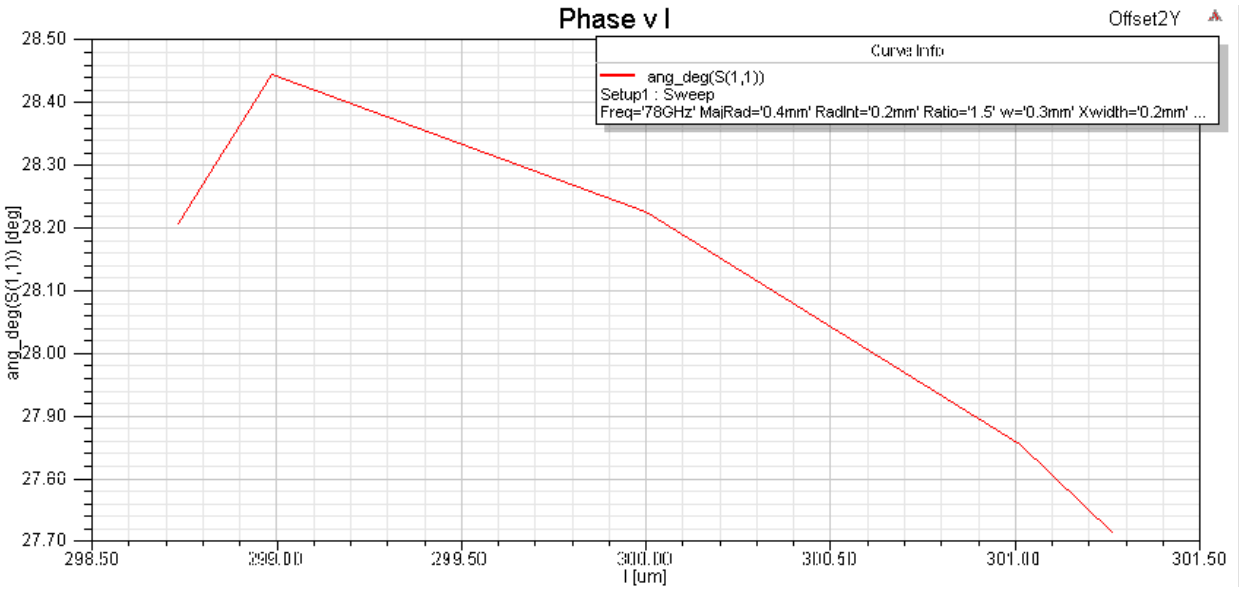

Figure 45: Sweep for l for the 315° zone patch

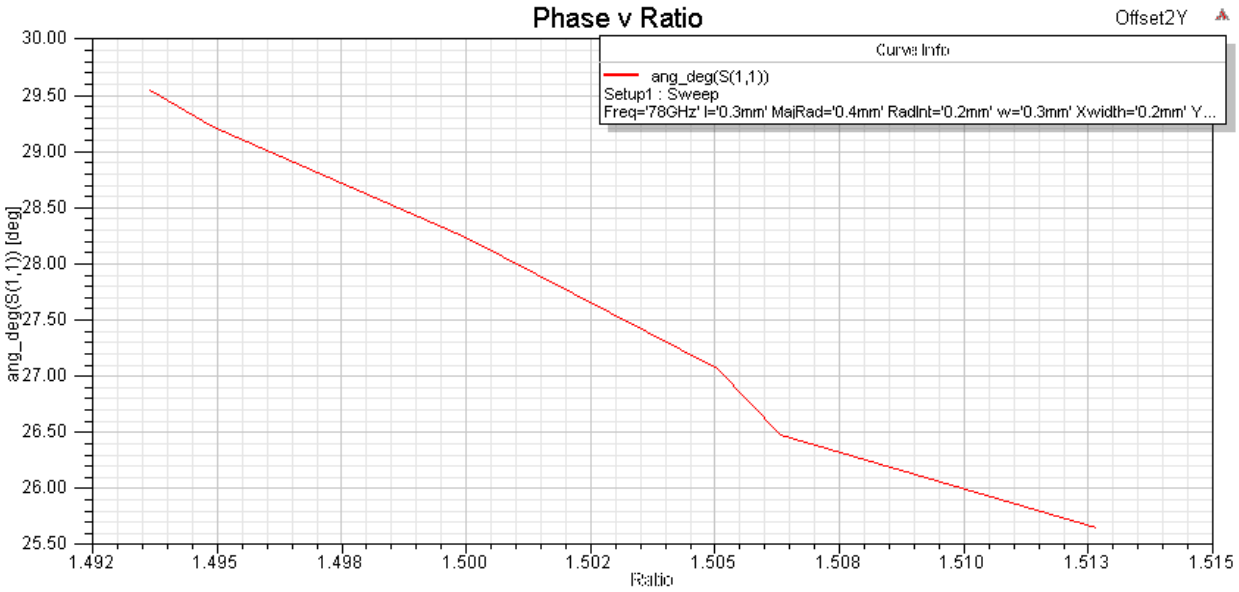

Figure 46: Sweep for Ratio for the 315° zone patch

Table 2: Dimensions for the 0° zone patch

0° Zone Patch	
CuRad	0.92 mm
W	0.5 mm
H2	0.8 mm
W2	1 mm

Table 3: Dimensions for the 45° zone patch

45° Zone Patch	
X1	1 mm
X2	0.2 mm
X3	0.4 mm
Y1	0.3 mm
Y2	0.1 mm
Y3	0.1 mm

Table 4: Dimensions for the 90° zone patch

90° Zone Patch	
R_ext	0.31 mm
R_in	0.3 mm
Height	0.4 mm

Table 5: Dimensions for the 135° zone patch

135° Zone Patch	
CuRad	0.75 mm
delX	0.1 mm
delY	0.325 mm

Table 6: Dimensions for the 180° zone patch

180° Zone Patch	
Xmain	1 mm
Ymain	1.2 mm
Xlittle	0.2 mm
Ylittle	0.4 mm

Table 7: Dimensions for the 225° zone patch

225° Zone Patch	
R_ext_x	1.7 mm
R_ext_y	1.11 mm
R_in_x	1.2 mm
R_in_y	0.6 mm

Table 8: Dimensions for the 270° zone patch

270° Zone Patch	
MajRad	0.38817814 mm
RTh	0.1014334 mm
W	0.1985433 mm
L	0.19221895 mm
Ratio	1.46278216

Table 9: Dimensions for the 315° zone patch

315° Zone Patch	
MajRad	0.40280072884791 mm
RadInt	0.20003968336782 mm
Ywidth	0.70007298119324 mm
Xwidth	0.20004549004623 mm
L	0.30068271737023 mm
w	0.29991930987347 mm
Ratio	1.5278959790801 mm

The dimensions for each of the patches can be found in Table 2 through Table 9. The geometric variables are defined in Figure 3 through Figure 10.

The results from the simulations of the unit cell antennas can be found in Table 2. This table also compares the results gained from this paper with the results found in [**9**].

Table 10: Results and comparison with [**9**]

Fresnel Zone		0°	45°	90°	135°	180°	225°	270°	315°
Actual Phase	Results	-95°	-52°	-3°	41°	84°	130°	176°	-158°
AR (dB)	Result	0.3	0.23	0.11	0.37	0.42	0.12	0.77	0.9
	[**9**]	0.4	0.6	0.6	0.14	0.5	0.07	0.33	0.22
$\Delta\Phi^o$	Result	89	91	95	88	89	92	105*	108*
	[**9**]	89	86	89	89	93	90	88	92

As can be seen, the results from the simulations are similar except for the last two patches. When considering the overall results, the discrepancies in the simulation results between this paper and [**9**] could come about from having different geometries. As well, the literature results had the additional constraint of a minimum dimension of 100 μm. This minimum dimension restraint was not followed within this paper's simulations.

The last two patches, the 270° and 315° zones, are the more interesting ones to talk about. These patches are the two offset patches that the paper describes. The authors discuss that the offset was important to changing the reflected phase of the patch. The difficulty with this patch was the way in which it was simulated. Because the patch was simulated within an infinite periodic array, the patch was in the center of a unit cell $\frac{\lambda}{2}$ square even when offset. These last two patches have no additional information about them in the paper.

Since [**9**] fabricated the PRA, it is prudent to discuss the potential effects of fabricating and testing an antenna with these patch designs. The overall efficiency of the antenna would decrease, as the circular polarization of the elements is not uniform.

It has been noted previously that axial ratio in this paper has a different definition than is common when describing antennas. This redefinition is potentially to describe the intended effect of generating a uniform plane wave reflection, since if the axial ratio were 0 dB the minimum and maximum field would be the same magnitude.

E. Conclusions

The reflectarray antenna has had an interesting history. The original idea emerged in 1963 [**3**], but was ignored by industry until the rise of the microstrip antenna, leading to a patent in 1987 [**2**]. From then on the planar reflectarray was studied while in comparison to the parabolic dish antenna. Eventually, it gained use in research as a possible on-board radar antenna for helicopters [**9**], and eventually culminating in potential use in foreign object debris detection on runways [**8**]. The study using a PRA as a possible on-board radar antenna for helicopters stood out because it was one of the few to use dissimilar, meaning not just a small change in the geometry of a patch, shapes for the different reflection phase requirements.

This paper was intended to recreate the simulation results from [**9**]. This meant the design and simulation of eight separate patches in Ansoft-HFSS. To speed up the simulation time, the supercomputer maintained by the AHPCC was used. The final results showed that the final patch designs match up well to those found in [**9**], except for the last two. The discrepancy may be due to the simulation method used to simulate offset patches.

4. Works Cited

[1] Warren L. Stutzman and Gary A. Thiele, *Antenna Theory and Design*, 3rd ed. United States of America: John Wiley & Sons, Inc., 2013.

[2] R. E. Munson, H. A. Haddad, J. W. Hanlen, and Colo. all of Boulder, "Microstrip Reflectarrayfor Sattelite Communication and Radar Cross-Section Enhancement or Reduction," Antenna 2,684,952, August 4, 1987.

[3] D. G. Berry, R. G. Malech, and W. A. Kennedy, "The Reflectarray Antenna," *IEEE Transactions on Antennas and Propagation*, vol. 11, no. 6, pp. 645-651, November 1963.

[4] D. M. Pozar, S. D. Targonski, and R. Pokuls, "A Shaped-Beam Microstrip Patch Reflectarray," *IEEE Transactions on Antennas and Propagation*, vol. 47, no. 7, pp. 1167-1173, July 1999.

[5] D. M. Pozar, S. D. Targonski, and H. D. Syrigos, "Design of Millimeter Wave Microstrip Reflectarrays," *IEEE Transactions on Antennas and Propagation*, vol. 45, no. 2, pp. 287-296, February 1997.

[6] C. Han, C. Rodenbeck, J. Huang, and K Chang, "A C/Ka Dual Frequency Dual Layer Circularly Polarized Reflectarray Antenna with Microstrip Ring Elements," *IEEE Transactions on Antennas and Propagation*, vol. 52, no. 11, pp. 2871-2876, November 2004.

[7] B. D. Nguyen, J. Lanteri, J.-Y. Dauvignac, Ch. Pichot, and C Migliaccio, "94 GHz Folded Fresnel Reflector Using C-Patch Elements," *IEEE Transactions on Antennas and Propagation*, vol. 56, no. 11, pp. 3373-3381, November 2008.

[8] K. Mazouni et al., "77 GHz offset reflectarray for FOD detection on airport runways," *International Journal of Microwave and Wireless Technologies*, vol. 4, no. Sp. 1, pp. 37-43, February 2012.

[9] K. Mazouni et al., "Millimter Wave Circularly Polarized Fresnel Reflector for On-Board Radar on Rescue Helicopters," *IEEE Transactions on Antennas and Propagation*, vol. 58, no. 8, pp. 2763-2766, August 2010.

[10] B. Huder and W. Menzel, "Flat Printed Reflector Antenna for mm-Wave Applications," *Electronics Letters* , vol. 24, no. 6, p. 17, March 1988.

[11] A. Zeitler et al., "Folded Reflectarrays With Shaped Beam Pattern for Foreign Object Debris Detection on Runways," *IEEE Transactions on Antennas and Propagation*, vol. 58, no. 9, pp. 3065-3068, September 2010.

[12] K. Mazouni et al., "77 GHz FM-CW Radar for FODs Detection," in *Proceedings of the 7th European Radar Conference*, Paris, France, 2010, pp. 451-454.